NAVAL POSTGRADUATE SCHOOL

MONTEREY, CALIFORNIA

THESIS

TRIGGERED INFRARED EMITTER DISPLAYS FOR INDIVIDUAL IDENTIFY FRIEND-OR-FOE (IIFF) AND VEHICULAR MOUNTED IDENTIFY FRIEND-OR-FOE (VMIFF) DEVICES

by

Patrick S. Williams

June 2007

Thesis Advisor: Nancy M. Haegel
Second Reader: Richard M. Harkins

Approved for public release; distribution is unlimited

THIS PAGE INTENTIONALLY LEFT BLANK

REPORT DOCUMENTATION PAGE		Form Approved OMB No. 0704-0188

1. AGENCY USE ONLY *(Leave blank)*	2. REPORT DATE	3. REPORT TYPE AND DATES COVERED
	June 2007	Master's Thesis

4. TITLE AND SUBTITLE Triggered Infrared Emitter Displays for Individual Identify Friend-or-Foe (IIFF) and Vehicular Mounted Identify Friend-or-Foe (VMIFF) Devices	5. FUNDING NUMBERS
6. AUTHOR(S) Patrick S. Williams	
7. PERFORMING ORGANIZATION NAME(S) AND ADDRESS(ES) Naval Postgraduate School Monterey, CA 93943-5000	8. PERFORMING ORGANIZATION REPORT NUMBER
9. SPONSORING /MONITORING AGENCY NAME(S) AND ADDRESS(ES) U.S. Special Operations Command (SOCOM) Marine Corps Warfighting Laboratory (MCWL) Naval Postgraduate School Foundation	10. SPONSORING/MONITORING AGENCY REPORT NUMBER

11. SUPPLEMENTARY NOTES The views expressed in this thesis are those of the author and do not reflect the official policy or position of the Department of Defense or the U.S. Government.

12a. DISTRIBUTION / AVAILABILITY STATEMENT	12b. DISTRIBUTION CODE
Approved for public release; distribution is unlimited	

13. ABSTRACT (maximum 200 words)

Individual IFF devices, based on polymer emitters on flexible substrates, have been evaluated to determine range of activation and observation, performance under extreme environmental conditions, and emitter intensity decay as a function of multiple activations and time. Key results include observation at distances in excess of 700 meters and device functionality in a temperature range from -40 ^{0}C to 71 ^{0}C.

From data obtained in the development and testing of the individual anti-fratricide devices, a vehicle version is developed with the purpose of mitigating air-to-ground fratricide. A rudimentary prototype is developed and tested, followed by an improved, more powerful version. Field tests include establishing limits for activation and observability. Finally, the emission is captured and graphically represented as a function of time. Key results include observation at distances in excess of 9.5 km and demonstration of remote activation.

An area for further research using quantum dots down conversion is offered. Quantum dots down conversion could be used for wavelength tuning of the polymer organic light emitting material.

14. SUBJECT TERMS	15. NUMBER OF PAGES
Anti-fratricide, polymer organic light emitting display (P-OLED), individual identify friend-or-foe (IIFF), vehicular mounted identify friend-or-foe (VMIFF), night vision device (NVD)	93
	16. PRICE CODE

17. SECURITY CLASSIFICATION OF REPORT	18. SECURITY CLASSIFICATION OF THIS PAGE	19. SECURITY CLASSIFICATION OF ABSTRACT	20. LIMITATION OF ABSTRACT
Unclassified	Unclassified	Unclassified	UL

NSN 7540-01-280-5500

Standard Form 298 (Rev. 2-89)
Prescribed by ANSI Std. 239-18

THIS PAGE INTENTIONALLY LEFT BLANK

Approved for public release; distribution is unlimited

TRIGGERED INFRARED EMITTER DISPLAYS FOR INDIVIDUAL IDENTIFY FRIEND-OR-FOE (IIFF) AND VEHICULAR MOUNTED IDENTIFY FRIEND-OR-FOE (VMIFF) DEVICES

Patrick S. Williams
Captain, United States Marine Corps
B.S., Illinois Institute of Technology, 2001

Submitted in partial fulfillment of the
requirements for the degree of

MASTER OF SCIENCE IN PHYSICS

from the

NAVAL POSTGRADUATE SCHOOL
June 2007

Author: Patrick S. Williams

Approved by: Nancy M. Haegel
Thesis Advisor

Richard M. Harkins
Second Reader

James H. Luscombe
Chairman, Department of Physics

THIS PAGE INTENTIONALLY LEFT BLANK

ABSTRACT

Individual IFF devices, based on polymer emitters on flexible substrates, have been evaluated to determine range of activation and observation, performance under extreme environmental conditions, and emitter intensity decay as a function of multiple activations and time. Key results include observation at distances in excess of 700 meters and device functionality in a temperature range from -40 ^{0}C to 71 ^{0}C.

From data obtained in the development and testing of the individual anti-fratricide devices, a vehicle version is developed with the purpose of mitigating air-to-ground fratricide. A rudimentary prototype is developed and tested, followed by an improved, more powerful version. Field tests include establishing limits for activation and observability. Finally, the emission is captured and graphically represented as a function of time. Key results include observation at distances in excess of 9.5 km and demonstration of remote activation.

An area for further research using quantum dots down conversion is offered. Quantum dots down conversion could be used for wavelength tuning of the polymer organic light emitting material.

THIS PAGE INTENTIONALLY LEFT BLANK

TABLE OF CONTENTS

THIS PAGE INTENTIONALLY LEFT BLANK

LIST OF FIGURES

LIST OF TABLES

THIS PAGE INTENTIONALLY LEFT BLANK

ACKNOWLEDGMENTS

This work was supported through the joint research of the United States Special Operations Command (U.S. SOCOM) and Naval Postgraduate School (NPS) Cooperative Field Experiment Program. Also providing support was the Marine Corps Warfighting Laboratory (MCWL) and the NPS Foundation.

I acknowledge and appreciate the support and technical expertise of Sam Barone, Electronics Technician at NPS. He assisted me in building several electronic devices that substantially contributed to my research and completion of this thesis. I am also grateful for the support and technical work of Bill Cross, electrical engineer and owner of Syvax Design, Inc. Without his superior electronic design abilities and expertise, the creation of the final vehicular mounted anti-fratricide device would not have been possible. I extend a special thanks to Major Pavlos Andrikopoulos of the Hellenic Army, whose remarkable abilities to write code in MATLAB greatly helped me on numerous areas of this thesis.

A great deal of appreciation and thanks is also due to Matt Wilkinson and Dr. Devin Mackenzie, CEO and Director of Technology, respectively, at Add-Vision, Inc., whose state of the art work in polymer organic light emitting display (P-OLED) technology provided the basis for much of my testing and research. The idea for and creation of the original IIFF device is based on the operational experience of CDR F. Mitchell Bradley, USN, a previous NPS student working under the guidance of Dr. Haegel. The IIFF testing presented in this thesis is a continuation of CDR Bradley's work.

I owe the utmost gratitude and thanks to Dr. Nancy Haegel, my thesis advisor. Her tremendous amount of technical knowledge, combined with a strong work ethic, aided me greatly in my research and production of a finished thesis. She is by far one of the most outstanding persons I have ever met.

Finally, my beautiful wife Honey deserves thanks for the love and support she provided me while we were stationed at NPS. I love you very much.

THIS PAGE INTENTIONALLY LEFT BLANK

I. INTRODUCTION

A. FRATRICIDE DURING MILITARY OPERATIONS

Historically fratricide has been a problem for military commanders and plagued military operations with unnecessary losses. From the time of the Roman Empire to the current operations of Enduring Freedom and Iraqi Freedom, troops have inadvertently fired upon and killed or wounded one another. Fratricide, also known as friendly fire, is a term adopted by the U.S. military in reference to an attack on friendly forces by other friendly forces. Fratricide incidents fall into two categories: fratricide that occurs as a result of the "fog of war" and that which occurs as a result of intentional murder. The following discussion focuses on the former.

The "fog of war" is a phrase used to describe the level of ambiguity in situational awareness experienced by participants in military operations. Fratricide that occurs during the fog of war includes friendly fire incidents that occur under unintentional circumstances. It is caused by a number of things during battle, including physical ambient conditions such as smoke, dust, and darkness, as well as psychologically traumatic issues such as fear and uncertainty. Fog of war fratricide incidents fall into two categories. The first category involves error of position, where friendly fire aimed at the enemy ends up hitting other friendly forces. Such incidents were common during World War Two, where troops fought in close proximity to one another [1]. The second category of fratricide that occurs under fog of war conditions is errors of identification, where friendly troops mistakenly identify other friendly troops as the enemy. This is the most common type of fratricide during the high mobility and technologically advanced wars of the late 20th century and early 21st century [1].

It is true that as the complexity of warfare has grown, so have the percentage of fratricide incidents when compared to total casualties. During World War Two, 21,000 U.S. military deaths occurred as a result of fratricide [1]. Moreover, 21% of all U.S. casualties (killed in action and wounded in action) during World War Two occurred as a result of fratricide [2]. Fratricide was the

second highest ranking cause of death for U.S. troops during World War Two after killed in action by the enemy. The U.S. military experienced a similar percentage of fratricide incidents during the Korean War. During that war, 18% of all U.S. military casualties were a result of fratricide [2].

Towards the end of the 20th century, with the substantial advances in U.S. military technology and lethality and the decreasing number of U.S. troops killed by enemy fire, the relative percentage of fratricide incidents that occurred during U.S. conflicts and wars increased dramatically. During the 1991 Gulf War, 24% of all U.S. deaths occurred as a result of fratricide [1]. According to the Pentagon, at least 35 out of 148 American fighting men and women killed and 72 out of 467 Americans wounded during the Gulf War stemmed from 28 separate incidents of friendly fire. In percentage terms, this is a higher rate than in any other major conflict fought by Americans in this century [3].

Increases in the number of fratricide casualties as a percentage of total casualties are due, in part, to the sheer velocity of battle of modern warfare [3]. During the 1991 Gulf War, armored units moved day and night during the four day ground attack, covering tremendous distances. In a desert environment without identifiable terrain features, it is easy for units to get lost and unintentionally encounter and engage other friendly units [3]. In such cases, especially under less than ideal conditions such as darkness or reduced visibility, it is critical to the survival of forces to easily identify one another and engage in combat.

The problem of identification is exacerbated by the limitations of current identification measures [3]. Often troops manning modern day battlefield equipment such as tanks and rotary wing aircraft can shoot farther than they can see. In the Gulf War, visibility was often obscured by rain, sandstorms and the smoke from oil fires. At such great engagement distances, tank gunners looking through thermal sights and pilots using forward looking infrared (FLIR) technology to identify and designate targets, while flying at 200 mph, can easily mistake friend for foe.

As the U.S. military continues to maintain a technological superiority over its enemies, enemy fire becomes less of a problem. As a result, U.S. military deaths as a result of enemy fire have declined over recent wars. Deaths due to friendly fire incidents, however, have increased. This is a reflection of the way weapons systems have advanced faster than recognition capabilities [4]. In today's modern battlefield, a target can be hit before it is identified visually by the crew manning that particular weapons system. Since U.S. weapons are extremely accurate and lethal, the ability of those weapons to impact and destroy their targets, friend or foe, is almost guaranteed.

The bitter experiences of 1991 led the U.S. military to devote more energy to minimizing friendly fire [4]. These efforts may have helped reduce the fratricide numbers thus far in Afghanistan, where four of 31 Americans killed in action (or 13%) were victims of friendly fire [4]. Current technologies in place to prevent fratricide include strips of glow tape attached to personnel's uniforms and visible only through rifle optics and night goggles, and tiny Phoenix Beacons, attached to vehicles and soldiers, that emit a flashing thermal (3-5 micron) pulse visible only through thermal imagers [4]. The U.S. military has also acquired the improved AN/PVS-14 monocular night vision device and AN/PVS-15 binocular night vision goggles in attempt to provide troops with better near IR night vision devices (NVDs) that allow them to better survey potential targets [5]. Moreover, most U.S. military vehicles are now marked with thermal strips or flashing infrared lights, which show up prominently in the goggles and other sensors.

If the fratricide statistics from Operation Iraqi Freedom are combined with those from Operation Enduring Freedom in Afghanistan, less than one percent of soldiers killed in those conflicts thus far were victims of fratricide [5]. Military analysts say part of that success is due to the fact that the ambushes and roadside bombings of the insurgents are less complicated than large war maneuvers and are the cause for fewer friendly fire mistakes [5]. Technology, however, has also been a major contributor to the reduction in fratricide incidents. Many of the Army's Stryker vehicles, for instance, have onboard computer systems where friendly troops appear as thin blue circles

superimposed on a Baghdad satellite map [5]. This technology, however, is expensive and not easily employable on all military platforms. What is needed is a relatively inexpensive device that can be applied to all military platforms and is observable through current optics technology.

B. PURPOSE OF THESIS

The purpose of this thesis is to design, build, and test a triggered infrared vehicular mounted identify friend-or-foe (VMIFF) device to be used on military tactical vehicles to prevent low altitude, air-to-ground fratricide from airborne platforms. Specifically, the VMIFF was designed to prevent fratricide from the AH-1W Cobra helicopter, an airborne weapons platform currently in service with the U.S. Marine Corps. The results of the research, design, and production presented in this thesis will include two generations of the VMIFF and the results of design, testing, and evaluation conducted with each, including design schematics, maximum range observability, and light emitting diode (LED) spectral emission.

This thesis also summarizes the testing and evaluation of two generations of the individual identify friend-or-foe (IIFF) device built using polymer organic light emitting display (P-OLED) technology. Much of the basis for design for the VMIFF was developed from results from concurrent tests conducted on the IIFF. Results regarding maximum range observability, functionality under various extreme environmental conditions, and the variation of emitter intensity over time using a thermoelectrically cooled silicon charge coupled device (CCD) camera are presented in this thesis. Moreover, this thesis will also analyze the emission from the advanced target pointer illuminator aiming light (ATPIAL), a device currently in use by special operations forces of the U.S. military and manufactured by Insight Technology of Londonderry, NH. The ATPIAL provides a highly collimated beam of IR light (peak emissivity at wavelength of 830 nm) for weapon aiming and an adjustable focus IR beam for target illumination [6]. The device is used on such weapons platforms as the M4/M16 rifles, M249 squad

automatic weapon (SAW), M2 .50 caliber machine gun, and Mk-19 40 mm machine gun. It is relatively light in weight (7.5 oz) and extremely durable.

C. MILITARY RELEVANCE

Military convoy operations are essential to the movement of troops and materiel on the battlefield. Often the U.S. military seeks to conduct convoy operations under conditions of reduced visibility or in complete darkness. Historically, U.S. forces have held a monopoly on their ability to operate effectively and efficiently under the cover of darkness. In addition to ground forces, aircraft, both fixed wing and rotary, also conduct night operations, usually simultaneously and in close coordination with ground forces. The pilots of these aircraft use state of the art night vision devices (NVDs) and laser designating and targeting systems to identify, close with and destroy the enemy. In an area of operations where ground troops and aircraft are conducting joint operations, fratricide may result. This is especially true when aircraft must provide air support to friendly units who may be engaged in close proximity to the enemy.

The number of night operations the U.S. military conducts will only increase as technology improves our ability to identify and engage the enemy. An effective tool must be found to aid commanders in managing fratricide. The use of IR target designating lasers by U.S. military aircraft suggests the creation of a device to be mounted on U.S. military vehicles that will immediately and directly identify those vehicles as friendly as they are interrogated by the targeting laser, while maintaining a covert status otherwise. Practical constraints require that the device also be durable, low cost, reliable and provide operational security.

This thesis will outline the design, prototype, and testing of a unique type of combined sensor/emitter VMIFF system for military tactical vehicles. The prototype is designed for installation on two of the most numerous vehicle systems in the Marine Corps and U.S. military in general: the high mobility multi-purpose wheeled vehicle (HMMWV) and medium tactical vehicle replacement

(MTVR) 7-ton truck (Figures 1 and 2). At least one or both of these tactical vehicle systems would undoubtedly be found in any Marine Corps administrative or tactical convoy.

Figure 1. M998 HMMWV.

Figure 2. USMC MK23 7-ton Truck.

This thesis will also present the results of numerous tests conducted on the IIFF patch, designed to prevent small arms fire shooter-on-shooter fratricide.

This device, already in a third generation form, is a light weight, flexible device designed to be incorporated into an existing combat load and used in a tactical environment.

D. THESIS OVERVIEW

Chapter I provides an introduction to the thesis, examining the background that led to the need for the VMIFF, outlining the purpose of the thesis, as well the military relevance of the work. Chapter II characterizes the IIFF, a device that is a precursor to the VMIFF. Chapter II explains the necessity for the IIFF to prevent ground-to-ground fratricide, the technology and components that comprise the IIFF, as well as multiple laboratory and field tests and evaluations of the device. Chapter III characterizes the VMIFF. Chapter III includes an explanation of how the device will prevent fratricide from specific air-to-ground weapons platforms, as well as the design and testing of two prototypes. Also included in Chapter III are the experimental results of laboratory and field tests of the device. Finally, Chapter IV summarizes the results of the thesis and offers further areas for research and prototype development for the VMIFF.

THIS PAGE INTENTIONALLY LEFT BLANK

II. IIFF DEVICE CHARACTERIZATION

A. PRACTICAL APPLICATION AND DEVICE OPERATION

The conflicts of today involve numerous situations in which military personnel conduct operations under the cover of darkness and in relatively close proximity to one another. These operations are inherently dangerous due not only to the proximity of enemy forces, but also the likely chance of fratricide due to the proximity of friendly forces. Despite the inherent dangers of nighttime operations, the U.S. military will continue to conduct such operations due to their relative advantage over the enemy in night vision devices. Since most U.S. forces carry some sort of night vision device on their person as part of their prescribed battle load, it makes sense to also wear a device that when viewed through a NVD will positively identify friendly troops by the emission of radiation in the near IR wavelength (750 nm to 900 nm) region of the electromagnetic spectrum. Such a device, however, must be "smart" in the sense that it will only activate when interrogated by friendly forces. Due to the proliferation of NVDs and targeting lasers, a passive device that responds to interrogation from any laser or IR illuminating source is inherently risky due to the fact that it will respond to friend and foe alike.

The anti-fratricide devices proposed in this thesis will require few modifications of current equipment available in the military inventory nor any significant changes in standing operating procedures (SOPs) if they are adopted for use on the battlefield. Moreover, the devices are relatively easy to operate. Essentially, the devices are activated when interrogated by a modulated targeting laser or laser designator of a specific wavelength. At a sufficiently high modulation frequency, the laser will appear to be continuous wave (CW) to the operator as he scans the target through his NVDs. As the modulated laser radiation passes over the photodiode of the device, the device will respond by emitting a series of near IR pulses for the interrogator to view. The devices are smart in the sense that they will only pulse when interrogated with the proper wavelength radiation and modulation. Additionally, the devices are only on when

they are interrogated. The emitters remain in a standby mode until their photodiodes are illuminated with the proper wavelength signal at the prescribed modulation.

Due to research by previous students and in conjunction with Add-Vision, Inc. (AVI), of Scotts Valley, CA, such devices have been built and are currently in their third stage of prototype production. The generation 2 (G2) patch is powered by a non-replaceable 1.5 V coin cell battery. The generation 3 (G3) patch is powered by a replaceable 1.5 V AAA battery. The current patch is flexible and designed to be worn on the uniform, attached by Velcro. The flexible displays are integrated into a self-contained wearable patch that emits a flashing infrared warning signal when illuminated by a modulated encoded targeting laser, designed specifically for shooter-on-shooter IFF. Figure 3 shows the relative size of the G2 version of the patch when compared to a standard U.S. penny. The G2 patch has dimensions 4.25” x 2.88” x 0.125” (10.8 cm x 7.32 cm x 0.32 cm), while the actual emitter area of the G2 patch is 2.8 cm^2. In addition to being relatively small in size, the patch is also light, weighing only 68 grams.

Figure 3. Generation 2 IIFF patch.

When interrogated by a targeting laser from a friendly shooter, the device flashes back several pulses in the near IR to identify to the shooter that the target is a friendly. The patch was designed specifically to respond to the wavelength and modulation of the ATPIAL, a laser system currently in use by U.S. SOCOM forces. A photo of the ATPIAL displayed relative to a ruler is given in Figure 4.

Figure 4. ATPIAL System.

The G2 IIFF patch is turned on and off through the use of a magnet. The magnet's field in essence serves as a switch to activate the patch's circuitry. In such a form, the device is obviously not practical for operational military use. The patch must be turned off in order to preserve the battery, which in this case is a 1.5 V coin cell. When the patch is on, the microprocessor draws a small amount of current in "ready mode" as it is waiting to be interrogated. Since the G2 version was not designed with a replaceable battery, the patch has to be disposed of when the battery life expires. For this reason, it must be turned off when not in use.

The device in its current G3 version is easy to use and practical for military operational application. This is due to the fact that the G3 version uses a 1.5 V replaceable AAA battery and is equipped with an on/off switch. Moreover, the G3 version is not an extra burden to carry as it weighs only 79 grams. Additionally, the G3 version is dimensionally similar to the G2 version, with a length of 9.5 cm (11.5 cm with battery case) and a width of 6.5 cm (8.5 cm with battery case). As shown in Figure 5, the only noticeable difference between the G2 version and the G3 version is the AAA battery case and the slightly larger emitter area of the G3, which is about 3.4 cm^2.

Figure 5. Generation 3 IIFF Patch.

The G3 version is capable of operating in two modes: standby mode where it must be interrogated to activate, and continuous flash mode, where the emitter continuously flashes and acts as a beacon to reveal the wearer's position. Essentially, each soldier, marine, or SOCOM operator would wear two to four of these devices on his person as part of the prescribed battle load (Figure 6).

Figure 6. Generation 3 IIFF Patches Affixed to a Marine.

Each generation of the patch has been developed through the use of polymer organic light emitting display (P-OLED) technology developed by AVI. This unique, patented process prints numerous layers of P-OLED material onto flexible substrates. This device structure offers many of the attractive display characteristics of mainstream organic light emitting display (OLED) devices, but is much more easily manufactured [7]. The simplicity arises from the simplified

device structure, all layers being printable, and the use of flexible substrates [7]. Furthermore, AVI, through this unique process, has the ability to print custom emitter patters onto these flexible substrates. This approach therefore provides a combination of low cost and lightweight for this unique application. Although the emitters offer relatively low resolution, the brightness is sufficient for a range of display applications.

B. TECHNOLOGY AND COMPONENTS

The creation of electronic systems based on organic polymer materials has the potential to significantly lower the cost of electronic systems and provide for their application in an increasingly diverse range of environments [7]. Traditional constraints for inorganic based semiconductor electronics include the rigidity of the substrate materials and the costs of processing [7]. As mentioned above, AVI's unique ability to print polymer displays onto flexible substrates and develop emitter displays unique to specific applications allows for the creation of devices that are flexible, lightweight, ,and practical for military application.

AVI uses a special light emitting polymer (LED) ink that is doped with special additives and transport materials [7]. The specially formulated AVI LEP ink additives permit low voltage charge injection and high efficiency radiative recombination in the luminescent polymer without the need for vacuum deposited electrodes [7]. Moreover, AVI's doped P-OLED structure is much less sensitive to layer thickness than standard OLED technology. AVI's devices enable low voltage operation, high efficiencies, and uniform emission.

The G2 and G3 prototype IIFF patches (herein referred to as the "patch" for brevity) are based on a device structure that uses a yellow emitting P-OLED display filtered through a long pass IR filter that attenuates the visible emission. Figure 7 depicts the patented AVI layering process. First, indium tin oxide (ITO) is deposited as a contact layer on the plastic substrate. The covion yellow film is laid upon the ITO layer. Finally, a silver substrate backing is added to the film to serve as an electrical contact. A filter is placed upon the emission side to attenuate the visible emission for the specific IIFF patch application.

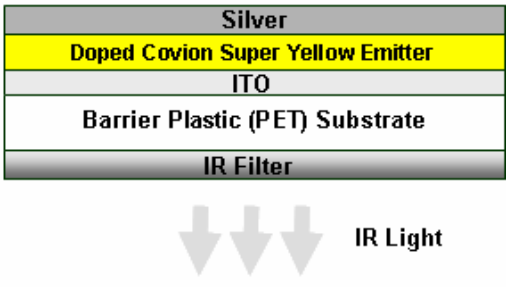

Figure 7. IIFF Generation 2 Structure with Covion Yellow (CY) and Long Pass Filter to Remove Visible Emission.

The resulting emission from the filtered device is only a small percentage of the P-OLED's spectrum (Figure 8). Measurements performed on prototype P-OLED devices and completed patches indicated that less than 5% of the emitted power of the P-OLED is observed in the IR. This is because the broadband yellow emitter is designed primarily for commercial, visible light applications.

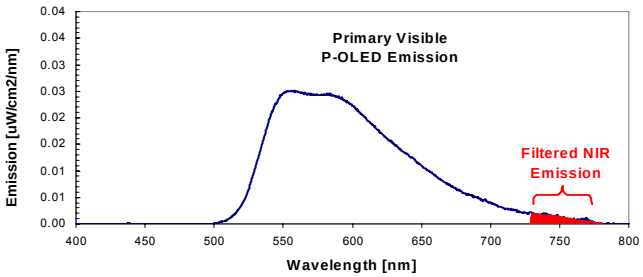

Figure 8. P-OLED Emission Spectrum.

The fact that 95% of the light emitted from the P-OLED is attenuated and not used in the practical function of the device as a near IR emitter indicates that the peak of the emission spectrum should be shifted to the IR so that the maximum amount of emission per unit of electrical power can be obtained. In graphical terms, this corresponds to more of the area under the curve (optical

power) emitted in the form of near IR radiation (longer wavelengths than the visible portion of the EM spectrum). This topic will be addressed further in Chapter IV.

Despite the optical power limitations, the G2 patch prototypes have been demonstrated to be observable to distances in excess of 350 m. The G3 patch, with an improved layering process and encapsulation method, as well as an increased emitter area, has been observed at distances in excess of 700 m. The optical power emanating from the emitter of the G2 version after it has passed through the IR filter is approximately 1-2 $\mu W/cm^2$.

C. TESTING AND EVALUATION

Over an eighteen month period, several laboratory and field tests were conducted on both the G2 and G3 IIFF patches. These tests included subjecting the patches to rigorous environmental conditions, exploring the relative drop in intensity over time of the emitter as a function of time and number of activations, and field tests where the patch was activated, observed, and filmed at various operational distances. The patch is activated by illuminating its photodiode with a laser designator that is modulated at a relatively high frequency. The peak wavelength of the radiation from the ATPIAL (the laser) is about 830 nm.

1. Emitter Intensity

Over a roughly one year period, one G2 patch was tested in the laboratory to determine how the intensity of the light from the emitter would decline as a function of time and number of activations. A G2 patch was mounted on the wall of a black, wooden box. A CCD camera was set up approximately one-half meter from the face of the patch. A neutral density filter was placed in front of the lens of the CCD camera. The patch was activated using an ATPIAL, and the integrated emission from a series of flashes was captured by the CCD camera and analyzed using the program MicroCCD 4. Each time the device was

illuminated with the ATPIAL, it flashed back five times (Figure 9). The CCD camera captured all five of the flashes and generated an integrated image based on the intensity of the flashes.

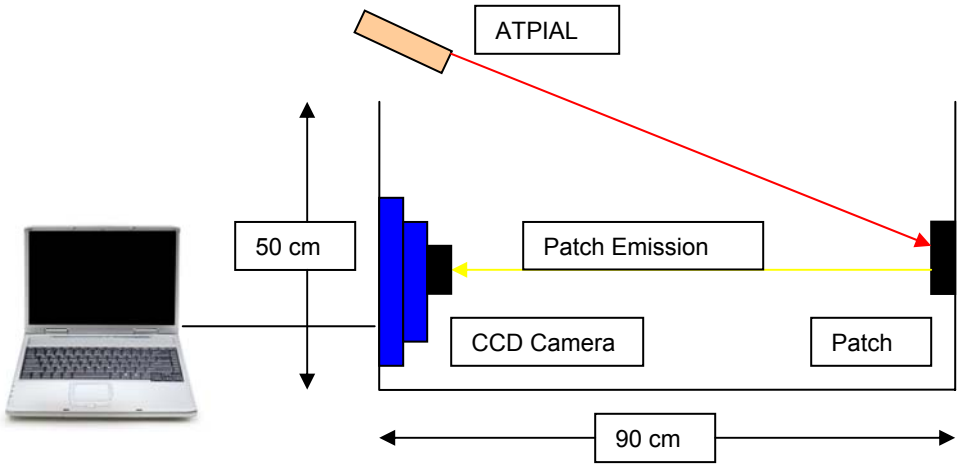

Figure 9. Schematic Drawing of Patch Intensity Testing Apparatus Enclosed in a Wooden Box (not to scale).

The above procedure was repeated twice a week for nearly one year. Two images were taken each time the experiment was conducted. The patch was activated four times prior to the images being captured by the CCD camera. This was done because it was discovered that the emission intensity remained relatively constant for each test period after four activations. This was due to the removal of the initial transient effects from the first few activation cycles. After the two complete images were taken and recorded by a laptop computer connected to the CCD camera, the emitter area was isolated from the rest of the patch through the use of the crop feature on MicroCCD 4. Each large 2184 X 1472 pixel image was cropped into a smaller 500 X 300 pixel image for intensity analysis. The line profile intensity feature was used at a constant value for each cropped image. For every test case, the line profile was set at y=120. The

intensity values were obtained for each leg of the chevron. Figure 10 shows an image of the G3 patch captured with the CCD camera. Intensity readings were taken at approximately the middle of each leg of the inverted chevron.

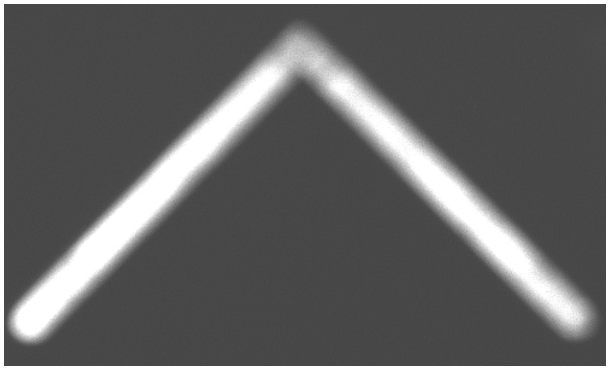

Figure 10. CCD Image of G3 Patch Emission.

Measurements were taken twice a week for the G2 patch over a nearly one year period. Figure 11 depicts the intensity of the emitter taken at the same, constant location on the first collected activation.

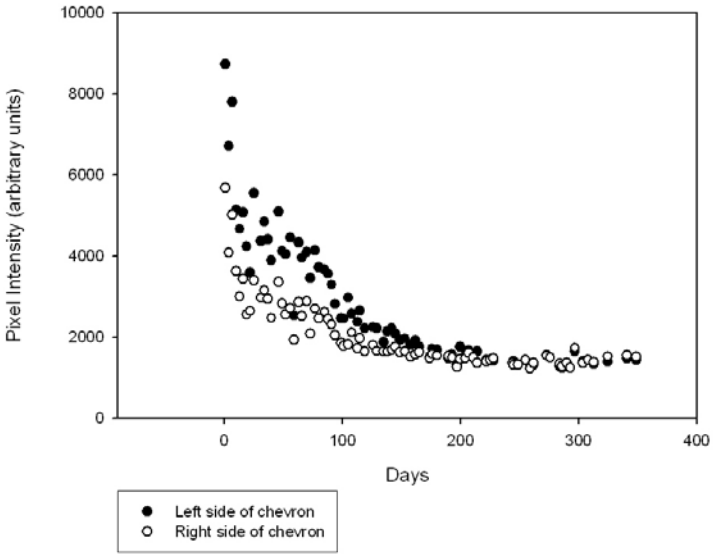

Figure 11. First Collected Exposure of G2 IIFF Patch, Intensity vs. Days.

As is evident from the plot of Figure 11, the intensity of the emitter decreased by a factor of approximately six over an almost one year period. In fact, the decay can be approximated as a decaying exponential. The equation for the decaying exponential used to best fit the data points from Figure 11 is given in the top right corner of Figure 12. The pixel intensity, I, is given as a function of the number of testing days, D.

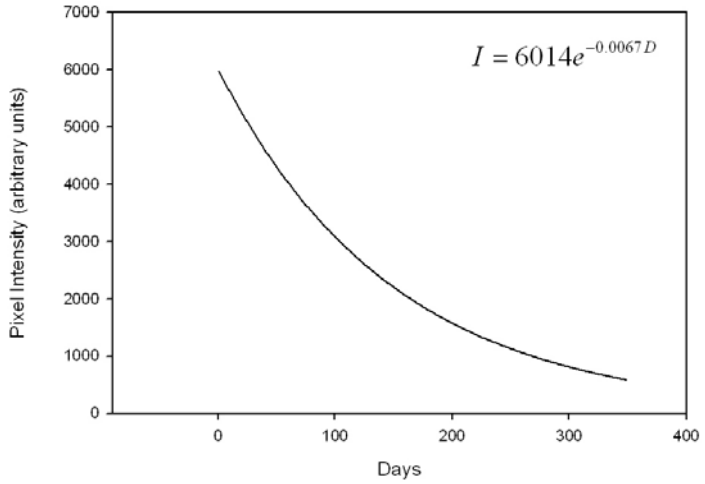

Figure 12. Exponential Decay Regression Curve of G2 IIFF Patch, First Collected Exposure, Left Side of Chevron, Intensity vs. Days.

The patch was tested over a 350 day period from 29 Dec 05 until 14 Dec 06. As the plot suggests, the average value of the intensity of the pixels at day 350 is about one sixth of that of the value at day 1 (1,000 vs. 6,000, respectively). Moreover, the left side of the chevron was, on average, brighter than the right side. During the course of the testing, it was observed that the relative intensity of the right side of the chevron did, in fact, decay faster over time than did the left side. Figure 13 is the plot of intensity vs. the total number of times the device was activated over a 350 day period. The plot in Figure 13 represents the same data as in Figure 10 but plotted as a function of activations rather than days. Figure 14 is a plot of the exponential decay regression curve used to fit the data with the equation for the curve given in the top right corner of the figure. This time, the pixel intensity, I, is given as a function of the number of activations, A.

Activation refers to the actual triggering of the device. Once the device is triggered, it flashes five times in a two second window for a flash rate of about 2.5 Hz. The device was triggered a total of 395 times for the first collected exposure test.

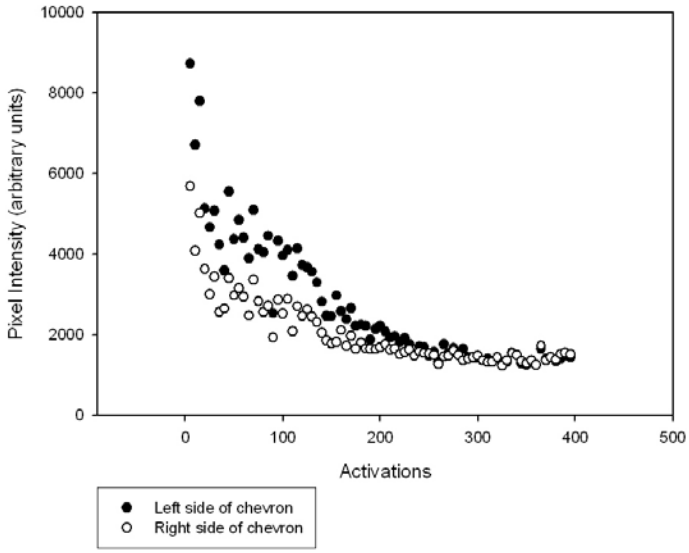

Figure 13. First Collected Exposure of G2 IIFF Patch, Intensity vs. Activations.

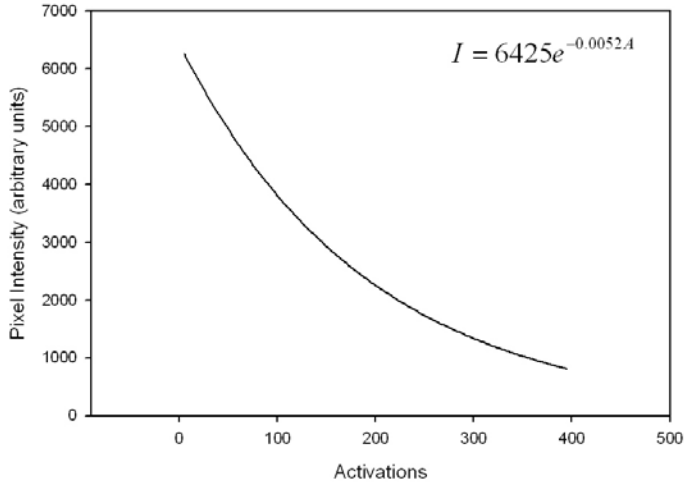

Figure 14. Exponential Decay Regression Curve of G2 IIFF Patch, First Collected Exposure, Left Side of Chevron, Intensity vs. Activations.

On average, each time the patch was tested, it was activated five times for the first collected exposure test: four times in a row to optimize the emitter

intensity and once for the first collected exposure test. As is evident by the plot in Figures 13 and 14, the intensity vs. activations is nearly identical to the intensity vs. days plot of Figures 11 and 12. The noticeable decay of the intensity vs. days and intensity vs. activations can most likely be attributed to a combination of decrease in power in the driver circuit as the battery is drained and moisture entering into the encapsulated emitter and affecting the behavior of the P-OLED material.

Figure 15 is a plot of pixel intensity vs. days for the second collected exposure of the patch. The exponential decay regression was omitted due to the fact that the shape of the curve is nearly identical to those in Figures 12 and 14.

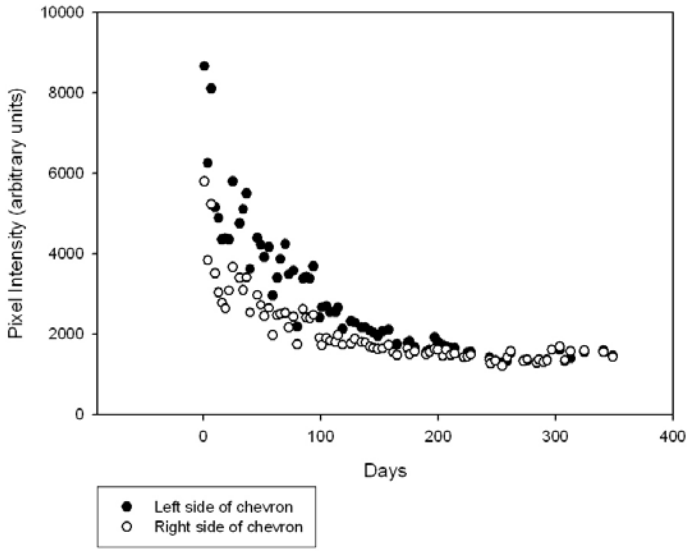

Figure 15. Second Collected Exposure of G2 IIFF Patch, Intensity vs. Days.

The plot for the second collected exposure of intensity vs. days does not vary significantly from the first collected exposure. The pixel intensity for the second collected exposure, however, was on average slightly greater than the first collected exposure for the same day. The plot in Figure 16 is of the pixel intensity vs. activations. This time, the average number of activations was six each time the patch was tested: four initial activations, one activation for the first

collected exposure and one activation for the second collected exposure. The device was activated 472 times for the second collected exposure test.

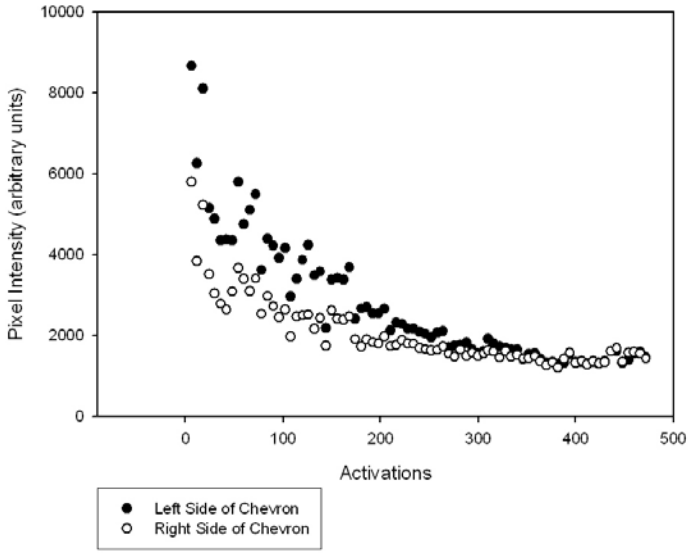

Figure 16. Second Collected Exposure of G2 IIFF Patch, Intensity vs. Activations.

It is evident from the plot in Figure 16 that the slope of the curve begins to level off at about 200 activations. Moreover, the pixel intensity of the left side of the patch and the pixel intensity of the right side of the patch are nearly equal at the 200 activation point. From Figure 15, it is apparent that the slope of the curve begins to level off at the 100 day mark. During the first 100 days of testing, the pixel intensity as a function of days decreased by a factor of four. After the 100 day mark, it approached a steady state value of intensity.

On 7 February 2007, a G3 patch was inserted into the same testing apparatus used to test the G2. The G3 patch was tested more frequently than the G2 patch, an average of five days per week, with a total of approximately six activations per test. Like the G2 patch test, two images were recorded per test day. The pixel intensity for the left and right sides of the chevron were recorded and plotted versus days and activations. This test was conducted until 4 April 2007 for a total of 68 days.

At day 61 of the test, the battery was replaced in the G3 patch and the tests conducted for an additional seven days. As is evident by the results in Figure 17, the pixel intensity for both the left and right side of the chevron demonstrates a steady decline up until the point where the battery is replaced at day 61, where there is a brief spike in intensity. After the initial intensity spike, however, the pixel intensity drops to a level of approximately the same value as before the battery was replaced, and continues to demonstrate an exponential decay behavior.

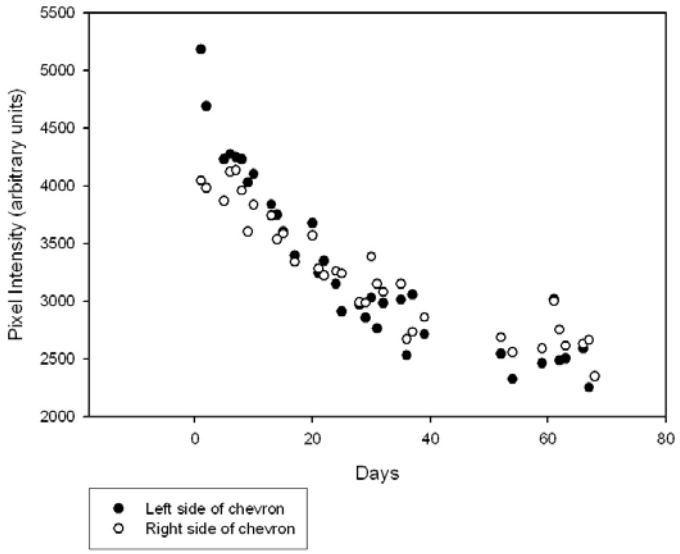

Figure 17. First Collected Exposure of G3 IIFF Patch, Intensity vs. Days.

The decay of the intensity of light emitted from the patch over a period of 68 days can be approximated with an exponential regression curve. This curve and its equation are given in Figure 18. It is evident by the curve that at day 60, the intensity of the emitter has dropped by about 55% of its original value, which is a better result than the decrease in intensity from the G2 patch tests.

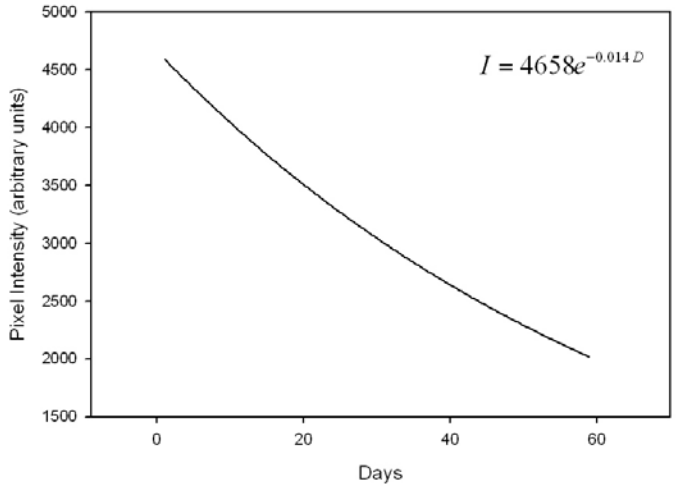

Figure 18. Exponential Decay Regression Curve of G3 IIFF Patch, First Collected Exposure, Left Side of Chevron, Intensity vs. Days.

This continuity in the intensity can be attributed to better encapsulation methods on the part of AVI and improvements in the P-OLED fabrication process. Figure 19 depicts the G3 patch's pixel intensity vs. activations and Figure 20 is a plot of the exponential decay regression curve of intensity vs. activations obtained from the intensity data for the left side of the chevron. The equation for the exponential decay curve is given in the top right corner of Figure 20 as in previous figures. This time, the pixel intensity, I, is given as a function of activations, A.

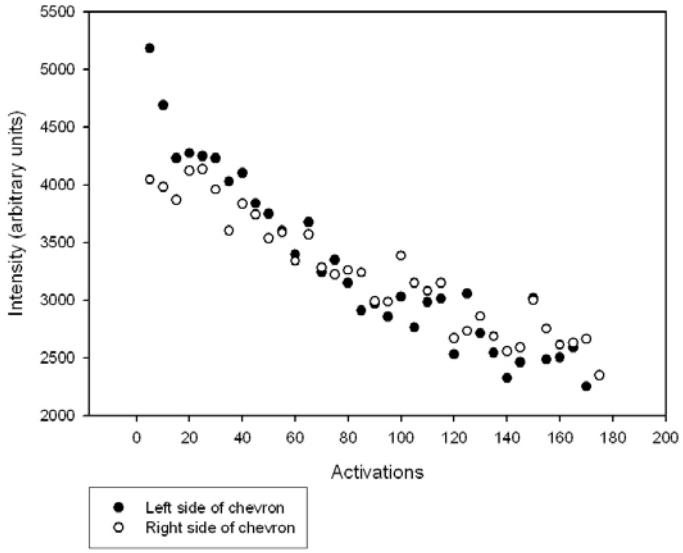

Figure 19. First Collected Exposure of G3 IIFF Patch, Intensity vs. Activations.

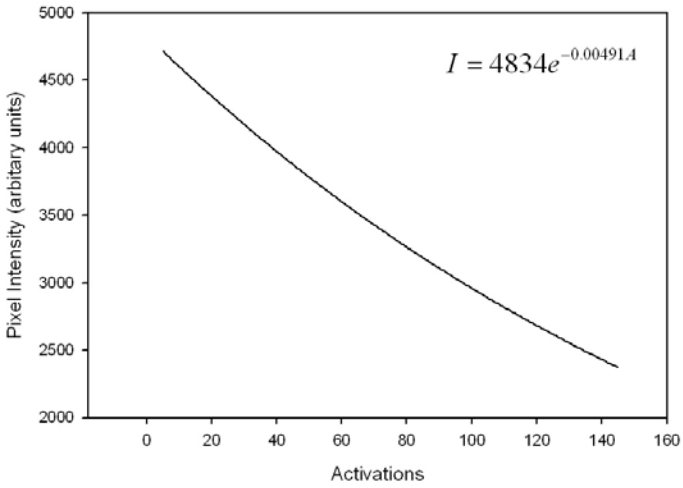

Figure 20. Exponential Decay Regression Curve of G3 IIFF Patch, First Collected Exposure, Left Side of Chevron, Intensity vs. Activations.

It is apparent from their respective slopes that the exponential decay regression curve of Figure 18 decays at a faster rate than that of Figure 20. Moreover, the pixel intensity at the 150th activation (Figure 20) is greater than the pixel intensity at the 60 day mark (Figure 18).

Figure 21 is a plot of the intensity vs. days for the second collected exposure of the G3 patch. As with the first collected exposure, an intensity value was obtained for both the left and right side of the chevron. On average, the intensity values for the second collected exposure are about the same as the first collected exposure. Moreover, as is evident by the exponential decay regression curve of Figure 22 for the second collected exposure intensity as a function of days, the intensity decays at about the same rate as the first collected exposure when measured as a function of days. That is, the slope of the exponential decay regression curve of Figure 22 is nearly identical to the curve slope of Figure 18.

The small peak in intensity on the plot of Figure 22 is due to the battery change at day 61. The intensity, however, at day 61 was only 3000, which is 64% of its original value of about 4700. Therefore, it is apparent that the decrease in emitter intensity is not due to just the battery drain, but is most likely due to material property and encapsulation methods, as stated previously.

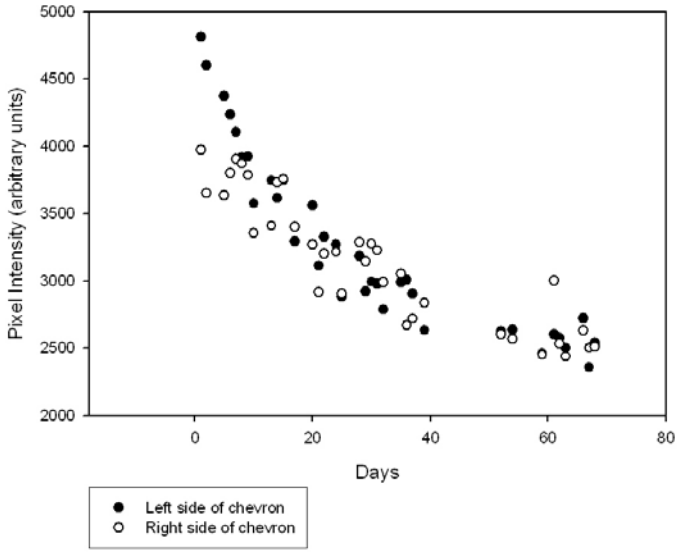

Figure 21. Second Collected Exposure of G3 IIFF Patch, Intensity vs. Days.

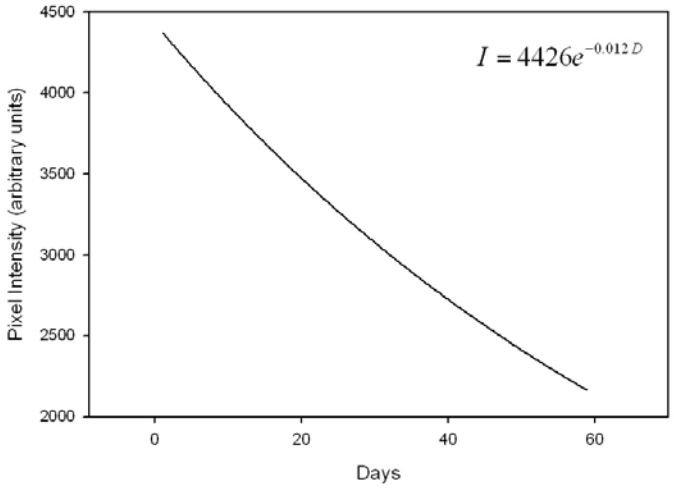

Figure 22. Exponential Decay Regression Curve of G3 IIFF Patch, Second Collected Exposure, Left Side of Chevron, Intensity vs. Days.

As with the first collected exposure of the G3 patch, the change in intensity as a function of activations for the second collected exposure was also measured and plotted. As is apparent by the data plot of Figure 23 and the slope of the exponential decay regression curve of Figure 24, the rate of emitter intensity decay when plotted over nearly 200 activations is slightly less than the rate of emitter intensity decay when plotted over a 60 day period. Moreover, the slope of the curve in Figure 24 is nearly identical to the curve in Figure 20. Consistently for G3 patch intensity tests, the rate of decay of the emitter intensity as a function of days has decreased between two and three times faster than the emitter intensity decay when measured as a function of activations.

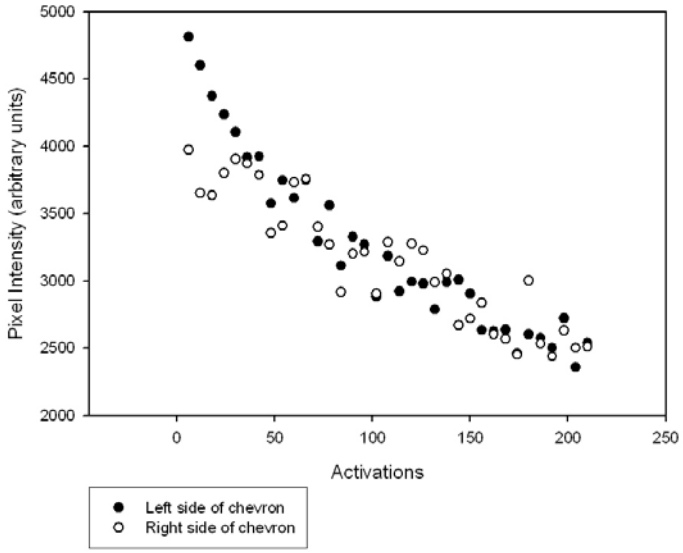

Figure 23. Second Collected Exposure of G3 IIFF Patch, Intensity vs. Activations.

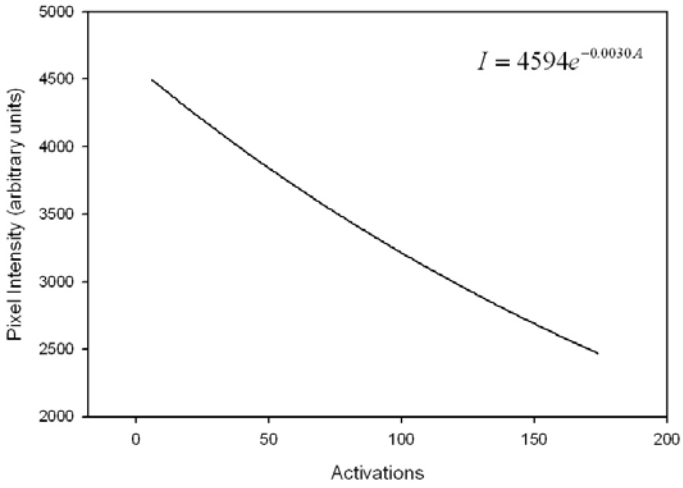

Figure 24. Exponential Decay Regression Curve of G3 IIFF Patch, Second Collected Exposure, Left Side of Chevron, Intensity vs. Activations.

In addition to determining the rate of decay of the emitter intensity of the G3 patch over a long period of time and a large number of activations, the rate of emitter intensity change over a relatively short period of time with continuous activation was determined. For this experiment, a new G3 patch was activated continuously for 21 activations over a period of five minutes. The intensity of the

left and right side of each chevron was obtained as per the procedures of the previous tests on the G2 and G3 patches mentioned above. For this experiment, however, the patch was not initially activated four times and data taken on the fifth and subsequent activations. Instead, data was taken on the first activation and continued until the 21st activation. Figure 25 is a plot of the emitter intensity as a function of activations for both the left and right side of the chevron. Included within the scatter plot of Figure 25 is a linear best fit curve along with its equation at the top right corner of the figure. The pixel intensity, I, is given as a function of activations, A.

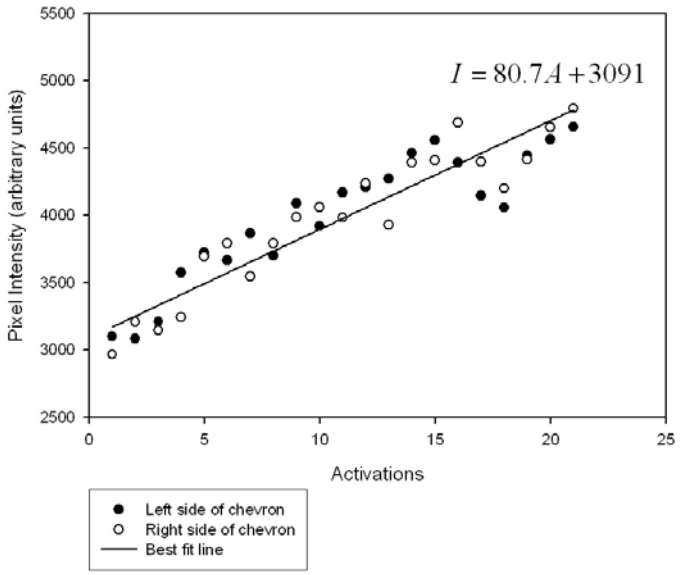

Figure 25. G3 IIFF Patch, Intensity vs. Activations, Continuous Activation.

It is apparent from Figure 25 that rather than decrease in intensity as the activations increase, the emitter intensity over a short period of time actually increased for both the left and right side of the chevron. In fact, the increase can be approximated as linear in nature as is evident by best fit line in Figure 25.

This trend of increase in emitter intensity for the first few activations was noted at the beginning of the G2 testing. As a result, each patch, both G2 and G3, was activated four times and exposures were collected for data analysis on the next two activations.

The long term trend of decrease in emitter intensity can be attributed to both the decrease in power supplied by the battery to power the emitter and the effect of the environment (e.g. moisture) on the material properties of the P-OLED. Further studies are planned to independently measure encapsulation and moisture effects.

2. Environmental Conditions

In addition to emitter intensity tests, both the G2 and G3 patches were subjected to a series of environmental conditions testing. It is imperative that a device used for military operations be able to withstand severe environmental conditions, including severe heat, severe cold, and exposure to water.

The initial tests were relatively benign in nature and were conducted on the G2 patch. The purpose of each test was to expose the patch to a certain environmental condition and then test it for functionality. The functionality portion of the test included turning on the patch, activating it with the ATPIAL, and observing the emission through the NVD. The first test on the G2 patch consisted of placing it inside a refrigerator at 34 ^{0}F (1.11 ^{0}C) for approximately one hour. The patch was taken out of the refrigerator and immediately moved to the test site (the entire move took less than five seconds), where the ambient temperature was room temperature (about 75 ^{0}F or 23.9 ^{0}C). The device was turned on by sweeping a small magnet across the back of the patch. The patch was then flashed with the modulated laser and observed through the IR goggles. The result of this first test was that a positive activation was observed from the patch with apparently the same approximate intensity as activation and observation under normal (room temperature) conditions.

The second test on the G2 patch consisted of placing the device inside a freezer at 5 ^{0}F (-15 ^{0}C) for approximately one hour. Similar to the refrigeration test, the device was taken out of the freezer and immediately moved to the test site (the entire move took less than 5 seconds), where the ambient temperature was room temperature (75 ^{0}F or 23.9 ^{0}C). The device was again turned on using a small magnet and then flashed with the modulated ATPIAL and observed

through the IR goggles. Once again a positive activation from the patch was observed with apparently the same approximate intensity as activation and observation under normal conditions.

The final initial test on the G2 patch was the submersible test to check for watertight integrity of the device. The patch was turned on, verified on by activation and observation through the NVDs, and placed inside a bucket of water at a depth of 7.67 inches (19.5 cm). The device was then flashed with the modulated laser while still submerged and observed through the NVDs. After the initial flash from the laser, the patch was kept submerged in the water for 15 additional minutes and tested. It was then tested for another 15 minutes at the 30 minute total submersion time. Finally, it was tested again after one hour of submersion. The total time the device was submerged was one hour. As with the other two tests, a positive activation from the patch was observed with apparently the same approximate intensity as activation and observation under normal conditions for all time intervals (i.e. instantaneous, 15 minutes, 30 minutes, and one hour). It was thus concluded that the G2 patch had watertight integrity at shallow depths.

In order for the device to be truly practical for military application, however, it needed to be subjected to extreme hot and extreme cold conditions. Both the G2 and G3 patches were subjected to such conditions through the use of a oven/freezer belonging to Laser Devices, Inc., of Monterey, CA. For both the heating and freezing tests, the G3 patch was inserted into the oven/freezer, left in for a specified time period, removed and activated four times, and put back into the oven/freezer. Table 1 summarizes the test data for the heating test.

Temperature (^{0}C)	Sub Duration (min.)	Total Duration (min.)	G2 functionality	G3 functionality
33	20	20	Yes	Yes
44	20	40	Yes	Yes
55	20	60	Yes	Yes
66	20	80	Yes	Yes
71	30	110	Yes	Yes

Table 1. G2/G3 Patches Extreme Heat Test Results.

As is evident by the results tabulated in Table 1, both the G2 and G3 patches withstood the measured temperature range. The temperature ranges were selected to most closely approximate the extreme conditions that U.S. military personnel may experience in an operational environment. The lower limit, 33 ^{0}C (90 ^{0}F) is on the mild side, where the upper limit, 71 ^{0}C (160 ^{0}F), is an extreme temperature that the device may be subjected to if locked inside of a container that was exposed to sun on an extremely hot day.

The next test conducted on the G2 and G3 patches was the extreme cold test. Table 2 summarizes the results of the cold test.

Temperature (^{0}C)	Sub Duration (min.)	Total Duration (min.)	G2 Functionality	G3 Functionality
0 ^{0}C	20	20	Yes	Yes
-17.8 ^{0}C	20	40	Yes	Yes
-40.0 ^{0}C	20	60	Yes	Yes

Table 2. G2/G3 Patches Extreme Cold Test Results.

As evident by the data in Table 2, both the G2 and G3 patches remained functional after exposure to a wide range of cold temperatures. From a mild cold of 0 ^{0}C (32 ^{0}F), to an extreme cold of -40 ^{0}C (-104 ^{0}F), both generation of patches

remained functional. Moreover, after each patch returned to equilibrium (room temperature) conditions for each test, they were again tested for activation and verified functional.

3. Maximum Range and Observability

A series of field tests were conducted on both the G2 and G3 patches over an 18 month period to determine the ranges at which the patches could be activated and the emission viewed through NVDs (Table 3). The majority of these tests were conducted at Camp Roberts, an installation devoted to training California National Guard troops aboard the larger military installation, Ft. Hunter Liggett. Camp Roberts was selected as a test site due to the ease of securing a training area there due to the fact that the testing could be incorporated into U.S. SOCOM sponsored tactical network training (TNT). Moreover, the large training area allowed for the ATPIAL to be used at maximum power and taken off of eye-safe mode. Table 3 presents a summary of the date, location, and measurements performed as part of the field tests conducted on both versions of the patches.

Test Date	Test Location	Patches Tested	Measurements
15 Aug 06	Camp Roberts (TNT site)	G2 and G3	Max activation range, emission intensity comparison
28 Oct 06	Camp Roberts (TNT site)	G3	Max activation, max range observability, video images from 100 m to 400 m
24 Feb 07	Camp Roberts (TNT site)	G3	High quality, focused video images of emission

Table 3. Summary of Field Tests Conducted on G2 and G3 Patches.

The following images were taken either on 29 October 2006 or 24 February 2007 during field tests of the G3 patch at Camp Roberts. The devices were activated and filmed using an Astroscope, a digital video camera fitted with an image intensifier tube to allow it to record video at night. Still images were cropped from the video footage at various ranges. In the figure below, the image is one of the G2 and G3 patch mounted side by side on the tailgate of a pickup truck. Both of the patches are activated to demonstrate the increased brightness of the G3 patch over the G2.

Figure 26. G2 (left) and G3 (right) Patches at 150 m.

In Figure 26, the G2 patch is mounted on the left corner of the tailgate while the G3 patch is mounted on the right corner. It is obvious that the G3 patch is considerably brighter than the G2.

The next series of experiments sought to find the maximum observable range of the G3 patch. This test was conducted by affixing two G3 patches to one side of a test subject and having that person move down range at 50 m to 100 m intervals. Figure 27 is an image of the activation of two G3 patches mounted to the front of a person as viewed through the Astroscope at 100 m.

Figure 27. Focused Image of Two G3 Patches at 100 m.

Once observability was confirmed, the test subject, contacted via hand-held radio, would walk down range 50 m to 100 m, stop and wait for the patches to be activated. Figure 28 contains images of the G3 patch as viewed from the Astroscope at 200 m. The image on the left includes the emission from the ATPIAL in the left hand corner of the image, while the image on the right is only of the emission from the patches.

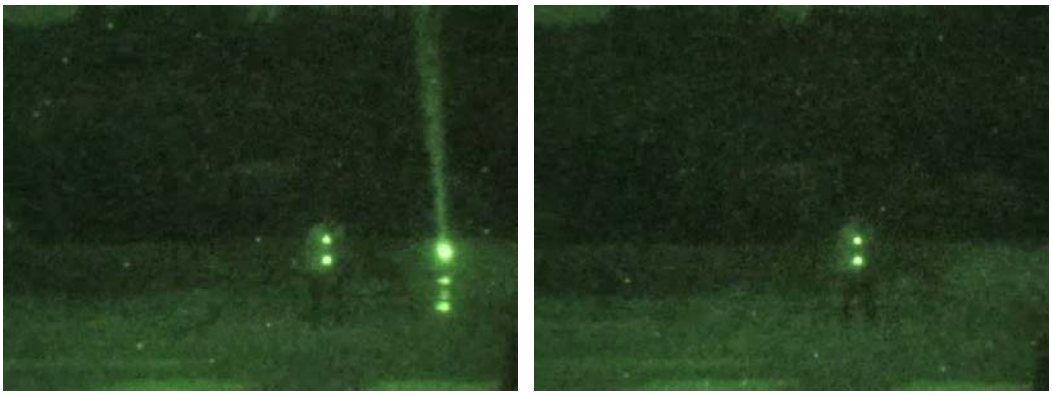

Figure 28. Focused Images of Two G3 Patches at 200 m.

Through the Astroscope, the patches appear nearly as visible at 100 m as they do at 200 m. This is due to the fact that the Astroscope was focused each time the patch emission was filmed. The above process was repeated until maximum range observability was achieved; that is, the patches were not visible through the AN/PVS-14s and AN/PVS-15s. At ranges in excess of 300 m, the

limit of visibility of the patches was beginning to be reached. Figure 29 depicts images of the G3 patches taken at 250 m and 300 m, respectively.

Figure 29. Focused Images of Two G3 Patches at 250 m (left) and 300 m (right).

At 350 m, the ability to see the patch through unaided (unfocused) optics began to become an issue. Figure 30 is an image of the two G3 patches as viewed through an unfocused Astroscope. The emission, though still strong, is difficult to distinguish.

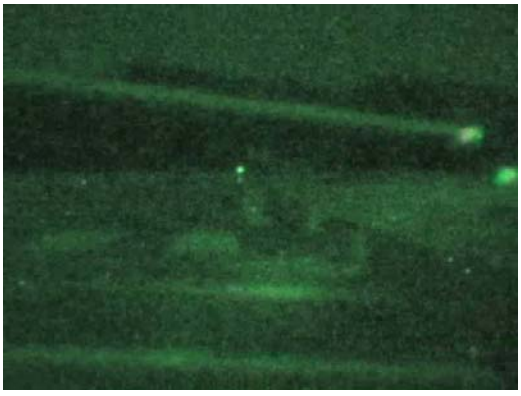

Figure 30. Unfocused Image of Two G3 Patches at 350 m.

In the above figure, the IR light source at the center of the image is the test subject with the activated patches on his back. The beam of light sweeping across the top of the image is the emission of the ATPIAL. The test subject continued to move at 50 m intervals out to 400 m. Figure 31 depicts focused images of the G3 patch taken at 350 m and 400 m, respectively.

Figure 31. Focused Images of Two G3 Patches at 350 m (left) and 400 m (right).

Range observability tests were also conducted on the G3 patch as part of a technology evaluation training exercise sponsored by SOCOM at Ft. Devens, MA, in November 2006 [8]. Along with the G3 patch, other anti-fratricide devices were tested. Some of these technologies used thermal emitter technology as well as near IR. Observers of the G3 patch reported observation out to 700 meters using AN/PVS-15B NVD.

4. NVD Spectral Response Measurement

The emission of the G2 and G3 patch is visible only through devices designed to respond in the near IR (750 nm to 900 nm) portion of the electromagnetic spectrum. Standard image intensifiers (known as NVDs for military applications) are based on the photoemission of a gallium arsenide (GaAs) cathode and therefore respond in the visible and near infrared. For the purposes of the IIFF and VMIFF testing, it is desirable to know the exact cutoff wavelength for image intensifying devices. In order to measure this, a spectral response measurement was made. The experiment was set up using a high intensity tungsten lamp supplied with 5 A at 13 V and dispersed using a monochromator. A 715 nm long pass filter was placed at the output of the monochromator. The filter allows only wavelengths in excess of 715 nm to pass, thereby filtering out all lower visible wavelengths, corresponding to the visible portion of the spectrum and eliminating second order effects. The output of the

monochromator was focused onto the surface of a stainless steel box. The initial wavelength was set at 750 nm and moved in increments of 0.80 nm/s. This emission was filmed using the Astroscope fitted with an image intensifying tube. The monochromator output was scanned from 750 nm to 1000 nm. Once the counter reached 1000 nm, the experiment was stopped, the monochromator was set again to 750 nm, and the experiment was repeated two more times.

The ultimate goal of this experiment was to create a series of digital images from the digital video stream of the decreasing intensity of the monochromator emission as viewed through the Astroscope as a function of wavelength. This would provide a system response of the NVD/Astroscope combination, with the cutoff wavelength associated with the NVD photocathode. In order to accomplish this, the digital video of the Astroscope was downloaded into a video editing program and digital images were cropped from the video at 15 second intervals. Each 15 second interval corresponded to a specific wavelength of the monochromator output. This series of images, converted to grayscale, with the brightness decreasing as the wavelength progressed towards 1000 nm, was loaded into MATLAB. Using MATLAB code created for this specific purpose (Appendix A), a value for the maximum intensity was extracted for its corresponding wavelength. This value, however, was not entirely accurate. For each image, MATLAB created a 640 X 480 pixel matrix. From that matrix, the MATLAB program extracted one value as the maximum intensity. Therefore, for a given image, the maximum value extracted by MATLAB could simply correspond to an arbitrary, illuminated pixel that may be from a reflection or outside light that does not in fact correspond to the actual output of the monochromator. Therefore, an averaging technique was used.

It was discovered that the minimum intensity in the full image area lay in the upper left hand corner of the image. A pixel matrix of 160 X 120 was chosen to sample this minimum value. It was also discovered that the maximum intensity of each image lay roughly 2/3 of the way across the image and 2/3 of the way down the image. Centered about a central point at those distances, a 160 X 120 pixel matrix was chosen to isolate the region of maximum intensity.

For both the matrix representing the minimum intensity and the matrix representing the maximum intensity, an average value of all 19,200 points was taken. The average minimum intensity (taken from the upper left hand corner of the image) was subtracted from the average maximum intensity in the region of interest to give a value that was used as the average maximum signal intensity of each image. This procedure was repeated for each image, corresponding to a specific wavelength. The signal intensity data were then plotted as a function of wavelength (Figure 32).

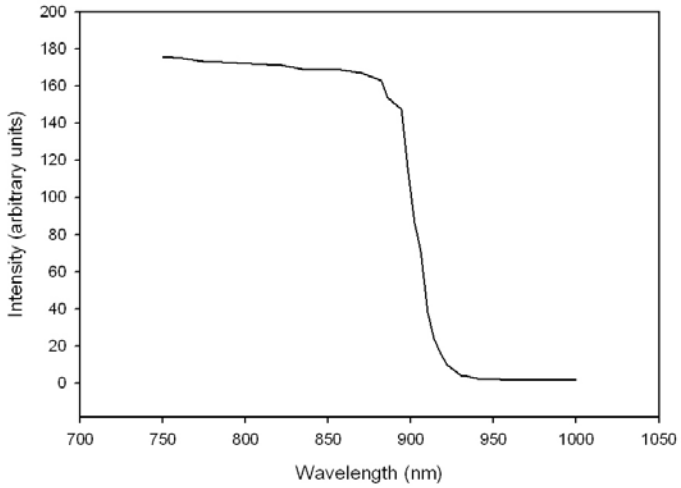

Figure 32. NVD Response vs. Wavelength.

As is evident by the plot of Figure 32, the intensity decreases slightly as a function of wavelength until about 900 nm. Past 900 nm, the intensity drops off rapidly as a function of wavelength. Clearly, then, it can be said that at wavelengths in excess of 900 nm, the intensity of a near IR image as viewed through an image intensifier experiences a significant decrease in image intensity.

It can be inferred from the NVD response vs. wavelength data that the optimized emission of an IR source must less than 900 nm in order to be visible through image intensifiers. For the IR, this corresponds to photon energies ranging from 1.38 eV at 900 nm to 1.65 eV at 750 nm.

In designing optimized polymer emitters (or light emitting diode (LED) sources) for observation with Generation 3 NVDs, the best emitter range is approximately between 750 nm to 875 nm.

THIS PAGE INTENTIONALLY LEFT BLANK

III. VMIFF DEVICE CHARACTERIZATION

A. WEAPONS PLATFORM APPLICATION

The current prototype of the VMIFF was designed to prevent air-to-ground fratricide from helicopterborne weapons platforms. Specifically, since the author is most familiar with USMC based platforms, the device was designed to respond to the testing parameters of the weapons systems of the AH-1W Cobra helicopter. The AH-1W model is armed with one 20 mm turreted cannon with 750 rounds, four external wing stations that can fire 70 mm or 127 mm rockets and a wide variety of precision guided missiles, to include TOW missiles (point target, wire guided), or Hellfire missiles (anti-armor, laser guided) [9]. Figure 33 is an image of the AH-1W Cobra attack helicopter.

Figure 33. AH-1W Cobra Helicopter in Flight Over the Atlantic Ocean.

The mission of the Marine light attack helicopter (HMLA) squadron is to provide offensive air support (OAS), utility support, armed escort, and airborne supporting arms coordination during naval expeditionary operations or joint and combined operations [10]. Support includes close air support against point and anti-armor targets, operating at night and under adverse weather conditions, and conducting armed escort. It is clear that inherent in the support missions of the Cobra helicopter are opportunities for fratricide to occur. Engaging targets at night or under adverse weather conditions, especially while performing the mission of armed escort, presents serious challenges to a pilot's ability to identify friend from foe.

Cobra pilots engage targets in several different ways. The techniques employed in the delivery of air-to-surface weapons will be selected by the pilot based on the tactical factors and conditions existing on the battlefield [10]. The Cobra may engage a target with diving fire, running (level) fire, hover fire, or by use of low-altitude pop-up fire. Running fire is delivered on target while the Cobra is in level, forward flight. It can be delivered from any altitude, provided the slant range to the target is less than or equal to the maximum effective range of the weapon [10]. This is the type of fire most likely to be used to strafe a convoy of vehicles.

Hover fire is delivered from a firing point with a known range to the target. It is most commonly associated with precision-guided munitions (PGM) employment but can be used to employ any weapon [10]. Hovering fire is the least accurate method to deliver rockets.

Diving fire is delivered on a target while the helicopter is in forward, descending flight. Diving fire is the most accurate type of fire for unguided ordnance. Unguided ordnance includes 20 mm canon rounds, and 70 mm or 127 mm rockets.

Finally, low altitude pop-up fire is used to deliver accurate ordnance from the low-altitude regime. This technique combines running fire and diving fire to give the AH-1W crew an accurate method of delivering fire from the low-level environment [10]. The pilot advances towards the target and at 1,500 to 2,000 meters away from the target the AH-1W “pops” up to an altitude of 300 to 600 feet (90 to 160 m) to deliver a nose down diving fire profile [10].

It is apparent from the different firing profiles of the Cobra that numerous opportunities for fratricide exist. Moreover, the numerous weapons systems on board the Cobra allow for the pilot to engage multiple targets at close or long ranges. Cobra pilots base target acquisition on a three step process: detection, recognition, and identification. Detection of a possible target may involve a thermal image of the target on the pilot’s forward looking infrared (FLIR) display screen. This is far different, however, than a positive identification before the target can be engaged. According to interviews conducted with Cobra pilots, a

military truck can be detected at approximately 5-7 km, while the truck can be recognized at 3 km to 5 km, and visually identified by the pilot inside 1 km to 3 km.

In order to engage the target the pilot must first know its range. Cobra helicopters are equipped with a laser range finder that provides the pilot with a 10-digit grid coordinate to the target [10]. On the older versions of the Cobra (N and W models), the laser designator is part of the night targeting system (NTS) designed by Kollsman, Inc. On the new versions of the Cobra (Z models), the laser designator is part of the target sight system (TSS) designed by Lockheed Martin. Using the either the laser ranging or laser designator systems of either the NTS or TSS, the pilot may engage the target with either unguided or guided munitions. Unguided munitions consist of rockets and guns, while guided munitions include Hellfire missiles. When using Hellfire missiles, the pilot must illuminate the target with a 1.06 micron Nd:YAG laser designator. The seeker head of the Hellfire missile is programmed to respond to a specific pulse repetition frequency (PRF) of the laser designator. The laser designator sweeps out a wide arc while illuminating the target. The seeker acquisition zone is within a 120-degree cone whose apex is at the target and extends 60 degrees on either side of the target to weapons line (TWL) [10]. Locating the laser designator within this cone ensures that sufficient reflected laser energy is received by the seeker and that the laser spot is not masked by the target. The optimal portion of this acquisition area extends to 45 degrees either side of the TWL [10].

It is true that it is not standing operating procedures (SOP) for a Cobra pilot to use the laser designator when employing weapons systems other than the Hellfire missiles. If the VMIFF device is incorporated into military operations, however, use of the laser designator prior to engaging a target at night with any weapons system may become SOP.

The VMIFF is designed for observability within the 3 km to 5 km window needed for a Cobra pilot to recognize a potential target. Moreover, the VMIFF is not designed to replace current SOPs used for recognition and identification of a target. Rather, the VMIFF is designed as a supplement to current SOPs to be

used as a last measure prior to engaging a potential target. The VMIFF is designed to respond to photon signal from the 1.06 micron Nd:YAG laser designator at a specific PRF (generally between 1-20 Hz). Project managers from Kollsman, Inc., and Lockheed Martin, designers of the NTS and TSS, respectively, provided important data as to exactly how the Nd:YAG laser of the NTS and TSS is modulated. The energy emitted from the designator is 80 mJ over a 20 ns pulse duration, corresponding to a power, P, equal to
P=80 mJ/20 ns= 4 MW. The designator emits approximately 20 such pulses over a one second time interval, corresponding to a PRF of about 20 Hz.

In principle, the tactical operations surrounding the use of the VMIFF are simple. During night operations, while flying on his AN/VIS-9 NVD, the pilot would lase the potential target with his laser designator. The wide divergence of the designator would ensure that the entire target would be illuminated with laser radiation. If the potential target flashed back with a series of near IR flashes, the pilot would know that the potential target was in fact a friendly and would not engage.

B. VMIFF GENERATION 1 DESIGN, PROTOTYPE AND TESTING

The initial design of the VMIFF was based on the specifications and data acquired while testing the G2 IIFF patch. From field testing data, it was determined that the range for unquestionable visibility for the G2 IIFF patch was 350 m. Therefore, the power output at the emitter of the G1 VMIFF was proportioned to the emitter of the G2 IIFF patch. The G1 VMIFF was designed in the lab using basic, off the shelf electronic circuit components.

1. VMIFF Generation 1 Design and Prototype

It is known from basic electromagnetic principles that when an EM wave propagates through free space, the radiation intensity at the detector falls off like $1/d^2$ from the source if the source is treated as a point source. In the limit of large distances as is the case with the VMIFF (d>>source diameter), the source can be approximated as a point source. From Chapter II, the intensity of the source of

the G2 IIFF patch was 1 μW/cm^2. The total area of the inverted "V" of the G2 IIFF patch is approximately 2.8 cm^2. As stated above, the maximum range at which the G2 IIFF patch was visible was about 350 m. Therefore, the intensity at the detector (night vision device through which the observer is observing) is proportional to

$$I_{\det} \propto \frac{(I_{emt})(A_e)}{d^2} \propto \frac{(1\frac{\mu W}{cm^2})(2.8cm^2)}{(350m)^2} \propto 2.29x10^{-8}\frac{mW}{cm^2} \quad (1)$$

In the above equation, I_{det} is the radiation intensity at the detection device (NVD), I_{emt} is the intensity of the radiation emitted from the patch, A_e is the surface area of the emitting portion of the patch, and d is the distance from the emitter to the observer. Using the value of 2.29 x 10^{-8} mW/cm^2 as the minimum intensity needed for observation, approximate value of the intensity needed for the VMIFF emitter to be observable at 4,000 m can be determined. Equation (6) below gives the ratio of the emitter intensity of the VMIFF, $(I_e)_{VMIFF}$, versus the emitter intensity of patch, $(I_e)_{IIFF}$, to determine how much brighter the VMIFF emitter must be than the IIFF emitter for visibility at 4,000 m. The below calculation assumes that the emitter area, A_e, is the same for both the VMIFF and IIFF. The calculation is simply meant to represent the order of magnitude of brightness needed for observability at 4 km.

$$\frac{(I_e)_{VIFF}}{(I_e)_{IIFF}} = \frac{\frac{(I_{\det})(d^2_{VIFF})}{(A_e)}}{\frac{(I_{\det})(d^2_{IIFF})}{(A_e)}} = \frac{d^2_{VIFF}}{d^2_{IIFF}} = \frac{(4000m)^2}{(350m)^2} = 131 \quad (2)$$

It is evident from the above equation that the intensity needed at the emitter of the VMIFF is 131 times greater than that of the IIFF, corresponding to a value of 0.131 mW/cm^2. For the design of the VMIFF, it was desirable to use a much larger emitter area than 2.8 cm^2. In fact, the dimensions of the top of the cab of a typical HMMWV are about 2.0 m x 0.90 m. Therefore, a larger emitter area is warranted. Initially, the emitter of the VMIFF was to be designed using the same P-OLED technology as was used for the G2 and G3 IIFF patches. It

was determined, however, that it would not be cost effective for AVI to manufacture such large emitter areas for the VMIFF prototype. Therefore, near IR LEDs were chosen as the source of radiation. Specifically, the Optek type OP265WPS LED was chosen (see Appendix B). This LED has a maximum aperture intensity of 0.55 mW/cm^2 and peak wavelength emission at 850 nm, which is ideal for observability through the AN/PVS-14, AN/PVS-15, and AN/VIS-9 NVD. Theoretically, one such LED would be visible at 4,000 m since the optical power output of the LED is four times greater than that needed for visibility at 4,000 m. It was determined, however, that using only a few such LEDs at such a great distance would most likely be indistinguishable from near IR background radiation. Therefore, it was decided to make the intensity of the G1 VMIFF emitter many times brighter than that which was theoretically needed for visibility. It was decided, based on the current and voltage requirements to power the LEDs, that a total of 85 of the Optek LEDs would be used, giving a total emitter intensity of

$$(I_{emt})_{VIFF} = (85)(0.55\frac{mW}{cm^2}) = 46.8\frac{mW}{cm^2} \tag{3}$$

This above value is about 350 times brighter than the estimated value for visibility at 4,000 m. Since the above calculations are only a rough estimate as to the intensity of radiation needed at the emitter for visibility at 4,000 m, it was determined that the device should be over designed to ensure that it would be visible through unaided NVD optics. Moreover, power consumption by the device is not an issue due to the fact that the HMMWV and MTVR each have two lead acid 12 V batteries.

As stated in Chapter II, both the G2 and G3 IIFF patches were designed to respond to 830 nm wavelength radiation modulated at a relatively high rate, which is characteristic of the emission from the ATPIAL. The G1 and G2 versions of the VMIFF were also designed to respond to the ATPIAL. Although the laser designator from the Cobra has a wavelength of 1.06 microns modulated at a PRF between 1-20 Hz, access to such a laser for testing was not practical.

Additionally, the initial purpose in testing the VMIFF was to achieve a maximum observation range, not a maximum activation range. As a result, the G1 and G2 versions of the VMIFF were designed to respond to a source present in the laboratory. The G3 version of the VMIFF, however, was designed to respond to the 1.06 micron wavelength of the Cobra's laser designator, modulated between 1-20 Hz.

The G1 version of the VMIFF, with much help from NPS electronics technician Sam Barone, was designed and built in the laboratory on a breadboard with stem type circuit components, to include resistors, capacitors, op amps, digital devices, and LEDs. The purpose of the construction of the G1 device was to develop a working device to test range observability, not create a device that could be immediately mounted to the roof of a tactical vehicle and taken to the field for use. As a result, the initial device, though functional, was relatively crude in nature.

The phototransistor selected for the G1 VMIFF was an Osram SFH314, with peak sensitivity at 850 nm. Figure 34 depicts the complete G1 VMIFF circuit schematic.

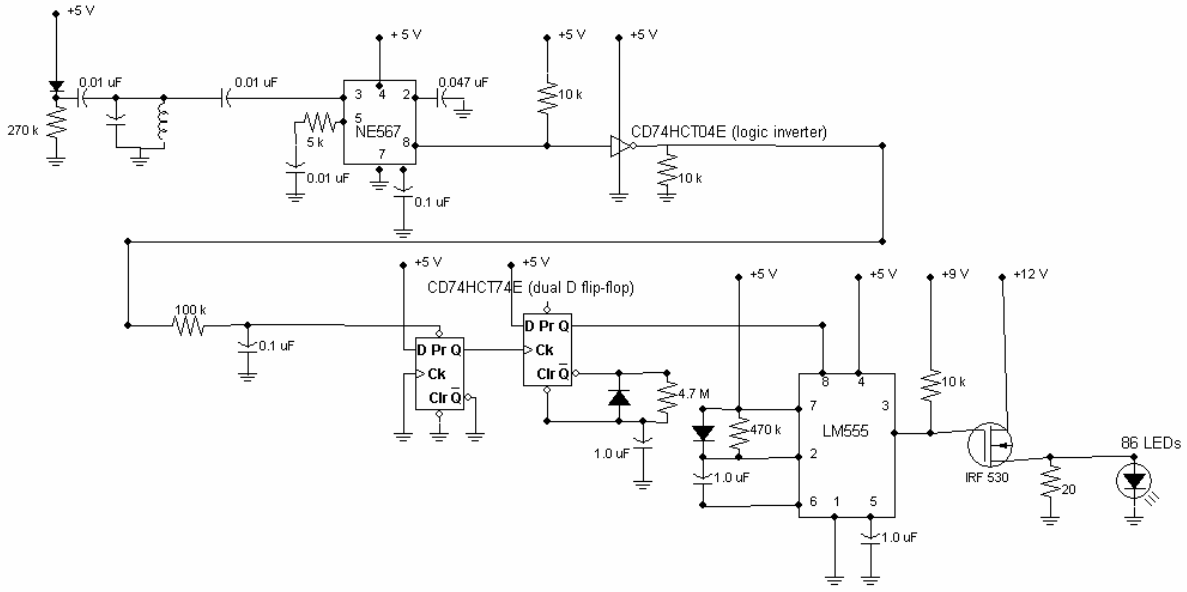

Figure 34. G1 VMIFF Circuit Schematic.

This phototransistor was selected for its relatively broad response spectrum (460 nm to 1080 nm), and its high collector current (50 mA). It was desirable to use a powerful phototransistor so that an op amp stage would not be needed to boost the current to power the circuit. The next stage of the device was an LC bandpass filter. The values for the capacitor and inductor comprising the bandpass filter shown in Figure 34 have been omitted for reason of security classification. As stated above, the G1 VMIFF was designed to respond to a modulated signal. Next, an NE567 tone decoder/phase-locked loop was used. This device is a highly stable phase-locked loop with synchronous amplitude modulation (AM) lock detection and power output circuitry. The output from the NE567 was a negative going pulse that was made positive after passing through the CD74HCT04E high speed CMOS logic hex inverter. From there, the pulse passes into a CD74HCT74E dual D-type flip-flop. The output from the flip-flop is a positive going pulse of width RC, in this case (4.7 MΩ)(1 μF)=4.7 seconds. In order to achieve the flashes from the LEDs within the 4.7 seconds pulse coming from the dual D-type flip-flop, it had to go through an LM555 oscillator. The LM555 oscillator was wired so that within the 4.7 second pulse provided by the dual D-type flip-flop, five flashes from the LED display would occur. Finally, the signal left the LM555 and passed into an IRF530 power metal oxide semi-conductor field effect transistor (MOSFET), where the current was stepped up to power the 85 LED display. The IRF530 transistor was powered by a 12 V DC source supplied by eight 1.5 V D-cell batteries. The logic circuit was powered by a 9 V battery.

The entire G1 VMIFF device was contained in a stainless steel box, measuring 17” x 10” x 3” (43.2 cm x 24.4 cm x 7.6 cm), spray painted black to reduce reflection (Figure 35). The LED displays were mounted using Velcro to the top of the box. They consisted of three small breadboards with approximately 29 LEDs on each one. Inside, another small breadboard was mounted using Velcro to an inner flange of the box (Figure 36). This breadboard contained the logic circuitry powered by a closely mounted 9 V battery. Finally, two small pieces of PVC pipe were cut to fit four D-cell batteries each. These were used to

power the 85 LED display. When activated, the LED display drew 1.2 A at 12 V. The device could be turned on and off by an external switch mounted to the side of the box.

Figure 35. Digital Image of G1 VMIFF LED Display.

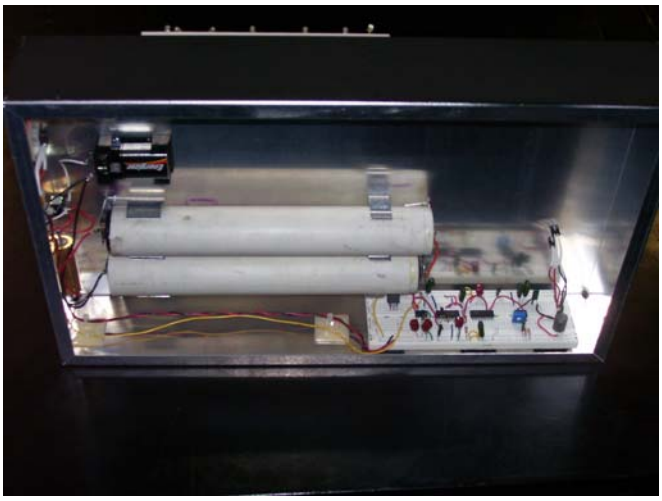

Figure 36. Digital Image of G1 VMIFF Logic Board and LED Power Supply.

2. VMIFF Generation 1 Testing

The G1 VMIFF was first tested in conjunction with G2 IIFF patch testing conducted at Camp Roberts on 15 August 2006. The G1 VMIFF was locally activated with the ATPIAL and visible at ranges up to 1,150 m. Images of the G1 VMIFF were taken, through the Astroscope, at ranges of 800 m (0.5 miles) and 1600 m (1.0 miles). The device was visible at these ranges, though the emission

was not as bright as anticipated. The emission from the G1 VMIFF is visible in the center of the images given in Figure 37. The 1600 m distance was chosen due to the fact that the runway ended at this distance and an image of the device's emission at a range near maximum was desired.

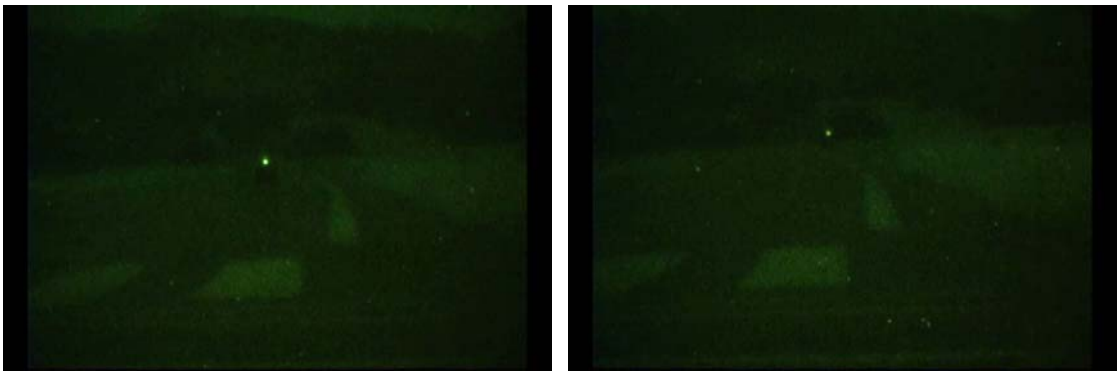

Figure 37. Images of G1 VMIFF at 800 m (left) and 1600 m (right).

The G1 VMIFF was not tested for visibility at 2,000 m due to the unavailability of a suitable location for observation at that distance, but was tested for visibility at 4,000 m. At this distance, the device was not visible through either the AN/PVS-14s or AN/PVS-15s. It was determined that the G1 VMIFF emitter was not emitting enough optical power to be visible at such distances. Therefore, a newer, more powerful version had to be designed and built to reach the goal of visibility at 4,000 m.

C. VMIFF GENERATION 2 DESIGN, PROTOTYPE, AND TESTING

The G2 VMIFF was designed by a professional electrical engineer and was much more powerful than the G1 VMIFF. As will be demonstrated by the data presented in the rest of this section, the G2 VMIFF was visible at distances in excess of 4 km (2.5 miles).

1. VMIFF Generation 2 Design and Prototype

The G2 VMIFF was designed to respond to the 850 nm high frequency modulation of the ATPIAL. The primary purpose of the G2 VMIFF was to obtain a maximum range of observation and obtain a maximum range of activation using the ATPIAL. A professional electrical engineering, Bill Cross of Syvax Design,

Inc., was hired to build the drivers and emitter display boards for the G2 VMIFF. The G2 VMIFF was built with sophisticated a sophisticated driver and high power Maurbeni L850F-06-55 LEDs. Each LED has a peak emissivity at 850 nm and emits 40 mW of radiated power (see Appendix C for LED specifications).

The G2 VMIFF was designed with five LED drivers controlled by one control unit. The entire circuit schematic of the G2 VMIFF, including controller and LED displays, is contained within Appendix D. Each LED driver powered 12 high power Marubeni LEDs (see Figure 38). Each time the device was activated by the ATPIAL, the controller sent a signal each LED driver to pulse its display for a total of five pulses. External leads led from the controller circuit board to a 12/24 V DC power supply. The entire device is able to run off of 12 to 24 V, with the current to each LED display at about 1 A. Therefore, for a total of five LED displays at 12 V, the total power is P=(5)(12 V)(1 A)=60 W.

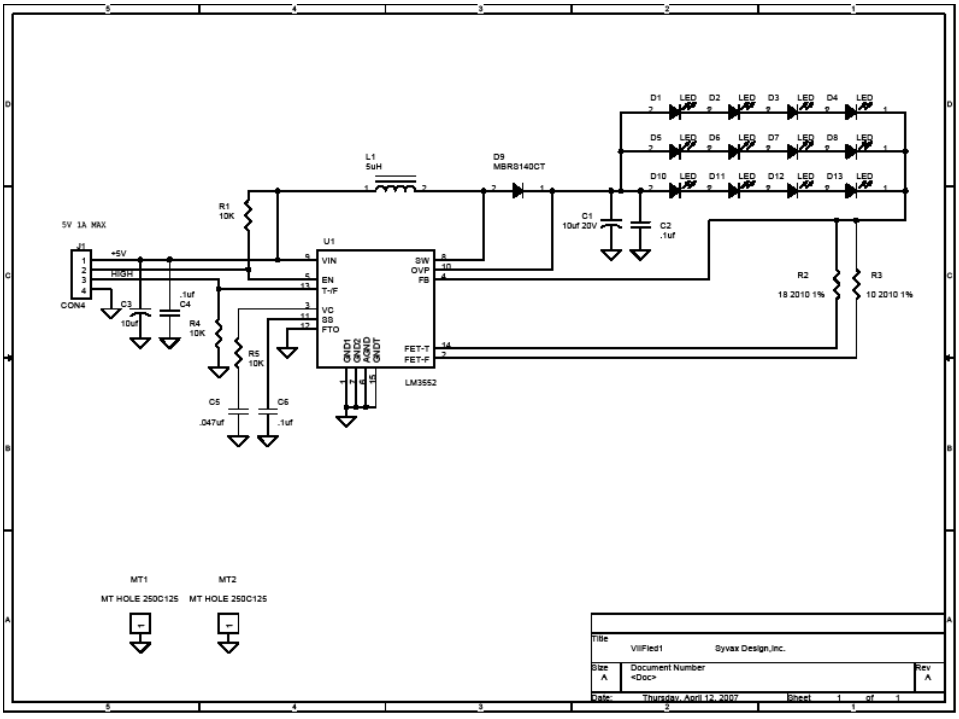

Figure 38. Schematics of LED Driver (courtesy of Bill Cross).

The circuit board that contained the controller and the LED drivers was small enough so that they could be encapsulated into a box that could easily fit

on the cab of a military tactical vehicle. Figures 39 and 40, respectively, are schematics of the controller circuit board and LED driver/LED circuit board. All dimensions on each schematic are in centimeters.

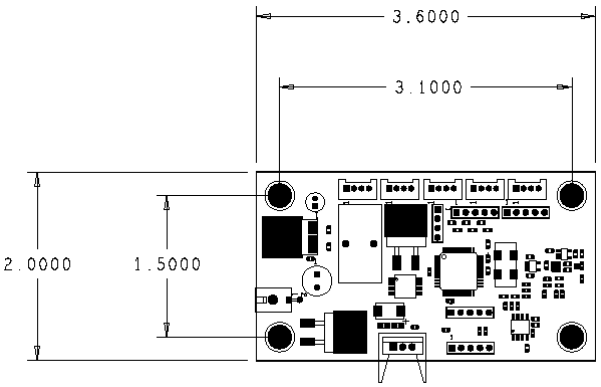

Figure 39. Controller Circuit Board Dimensional Drawing (courtesy of Bill Cross).

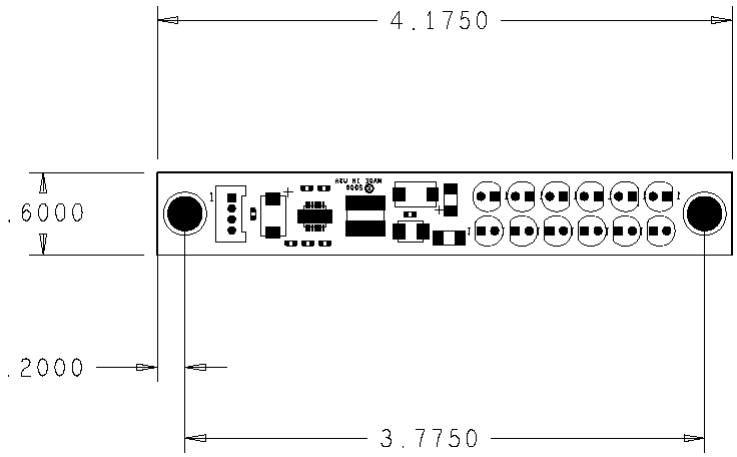

Figure 40. LED Driver and LED Circuit Board Dimensional Drawing (courtesy of Bill Cross).

The G2 VMIFF contains one of the controller boards displayed in Figure 39 and five of the LED driver/LED boards displayed in Figure 40. The boards are bolted into the underside of a 9.25” x 6.25” x 1.5” (23.5 cm x 15.9 cm x 3.8 cm) hard, black plastic box. Five rectangular slots are cut out of the top surface of the box to allow five displays of 12 LEDs each to protrude through the surface. A

not-to-scale schematic of the G2 VMIFF box with LED displays is given in Figure 41. A small 9 mm diameter hole covered with a 10 mm diameter half-ball lens was placed on the surface of the G2 VMIFF. The purpose of the half-ball lens is to focus laser light incident at various angles with respect to the surface of the device onto the photodiode.

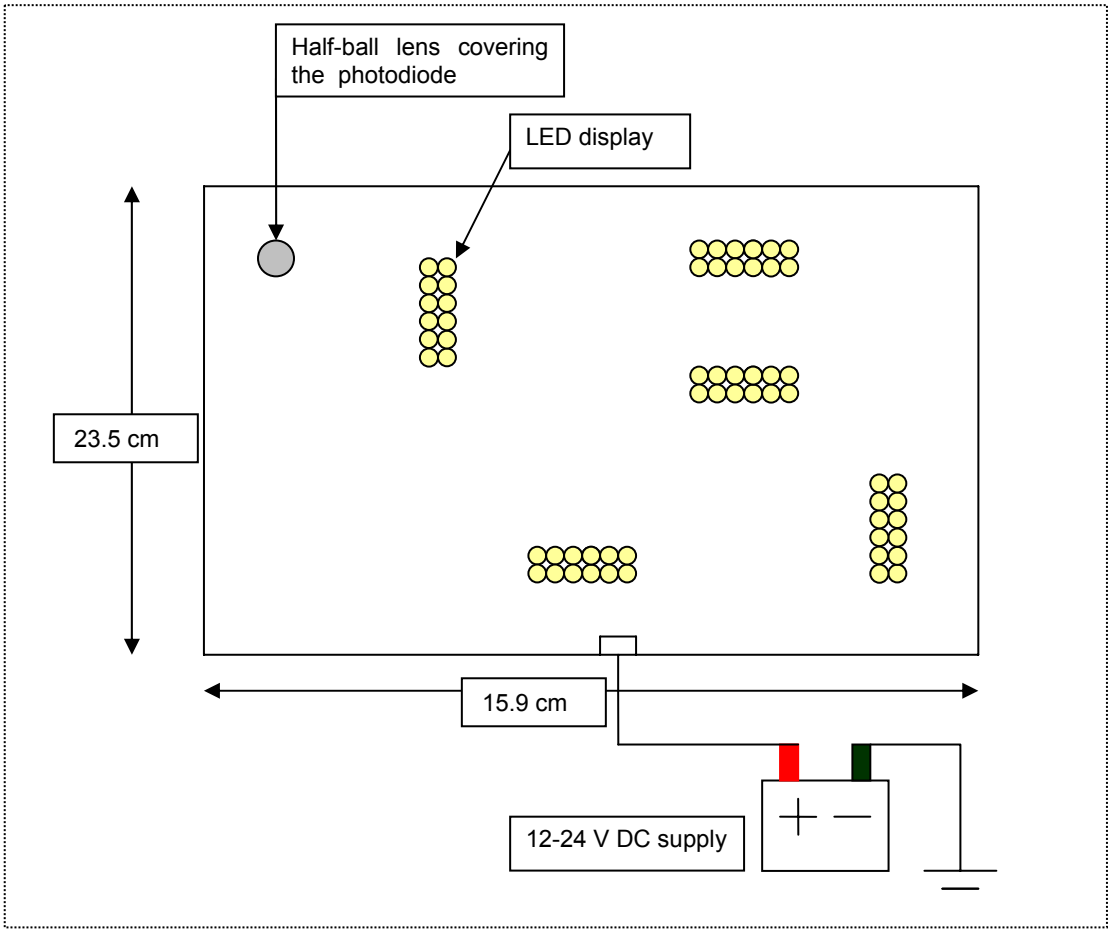

Figure 41. Dimensional Drawing of G2 VMIFF Box (not to scale).

The G2 VMIFF, as is evident by the schematic drawing of Figure 41, was powered by an external 12-24 V DC supply. During the field tests, this external supply was a 12 V rechargeable motorcycle battery (Figure 42).

Figure 42. Digital Images of G2 VMIFF with 12 V DC Power Supply.

The Images of Figure 42 depict the G2 VMIFF without the hemispherical lens (left) and with the lens (right).

2. VMIFF Generation 2 Testing

In order to achieve a time dependent measure of the emission of the G2 VMIFF, a simple operational amplifier (op amp) circuit was constructed. The operation of the circuit is relatively simple. The emission from the G2 VMIFF illuminates the photodiode. The current generated in the photodiode drives the op amp, whose output is connected to a digital oscilloscope. On the oscilloscope, the emission is represented on a voltage vs. time scale. Figure 43 depicts the simple circuit setup.

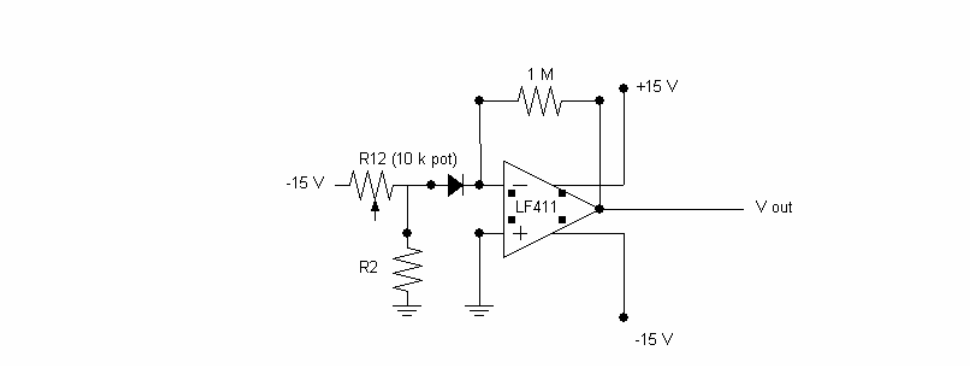

Figure 43. Op Amp Circuit to Capture Emitter Emission.

The circuit depicted in Figure 43 uses an LF411 op amp with a photodiode with a peak response to radiation at wavelengths of 850 nm. A 1 MΩ resistor is

used to connect the inverting input (pin 2) to the output (pin 6). Attached to the inverting input and running to ground is a 10 kΩ potentiometer. By adjusting the resistance on the potentiometer, the output voltage, Vout, can be controlled. The equation governing the resistance at R2 is given by the following:

$$10k\Omega - R12 = R2 \tag{4}$$

Additionally, the output voltage, Vout, is given by the following relationship:

$$V_{out} = (-15V)(\frac{R2}{R12} + R2) \tag{5}$$

For the purpose of emission spectra of the G2 VMIFF, R12 was set at 2 kΩ, thereby making R2=8 kΩ. It was discovered that these resistivities generated the best output at Vout. The voltage vs. time output of the G2 VMIFFis depicted in Figure 44.

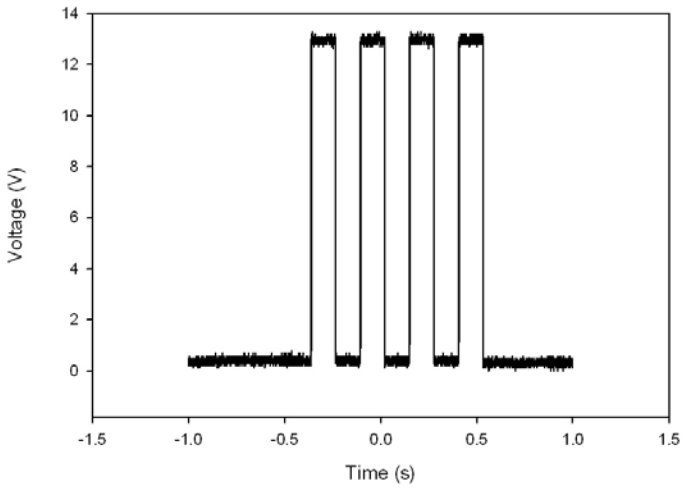

Figure 44. Voltage vs. Time Oscilloscope Plot from G2 VMIFF Emission.

The output is, as expected, in the form of a square wave with clear discernability between the up pulse (light emission) and down pulse (no light emission).

In addition to the laboratory test described above that was conducted on the G2 VMIFF, field tests were conducted on two separate occasions at Camp Roberts in conjunction with IIFF testing and TNT on 29 October 2006 and 24 February 2007. During the 29 October 2006 test, it was confirmed that the emission from the G2 VMIFF was visible through image intensifying devices at distances of 2 km (1.2 miles) and 4 km (2.5 miles). During the tests, the G2 VMIFF was set on top of a vehicle parked in the middle of the runway. The device was locally activated using the ATPIAL. The emission was viewed and recorded by the Astroscope from a hilltop overlooking the runway, first at a distance of 2 km and then 4 km (Figure 45).

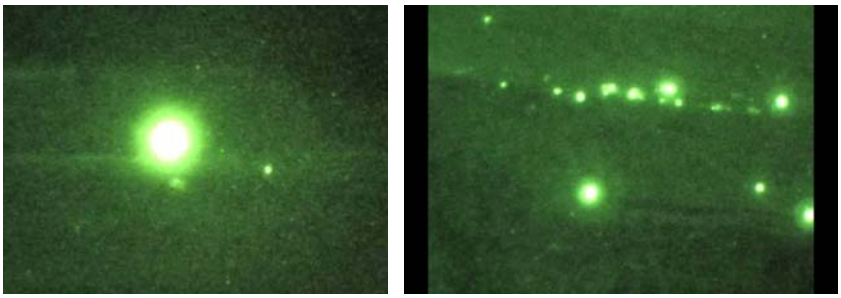

Figure 45. G2 VMIFF Emission at 2 km (left) and 4 km (right).

In the right hand image of Figure 45, the emission of the device is in the left center portion of the image. The other light sources in the image are ambient lights from the runway and training facility. The ambient light sources are displayed in the image to provide a frame of reference as to how bright the device is when compared to such sources. It should be noted, however, that in addition to the intensity of the emission, the device is also flashing to distinguish itself from the background.

On 23 March 2007, another field test was conducted on the G2 VMIFF at MCAS Yuma, AZ with Marine Air Wing Training Squadron One (MAWTS-1). For this test, a version of the G2 VMIFF was built to respond specifically to the emission from the laser designator of the Cobra's NTS. After information was obtained via conversations with the project managers from Lockheed-Martin, designers of the similar target sight system (TSS), a circuit was designed that is

responsive to the modulation from the laser designator of the TSS and similar NTS for the 23 March 2007 Yuma, AZ test. Nominal data are given in Table 4 below.

Parameter	Wavelength (μm)	Divergence Angle (mrad)	Energy per Pulse (mJ)	Pulse Width (ns)	Power (MW)	PRF Range (Hz)
Value	1.06	0.16	80	20	4.0	1-20

Table 4. TSS Technical Parameters.

The pulse repetition frequency (PRF) is the number of pulses per second. This is a variable rate that can be changed in both the helicopter's computer and on the seeker head of the Hellfire missile by the pilot. For the purposes of the Yuma, AZ, test, the PRF was known to be between 19-20 Hz. Due to cancellations in the training plan during the course of the Yuma test, the G2 VMIFF was not activated by the laser designator from the Cobra. Instead, a ground laser target designator (GLTD) was used to successfully activate the G2 VMIFF. The GLTD is used to illuminate targets from the ground in order to guide laser guided munitions until impact. The GLTD emits radiation with wavelength of 1.06 μm. Moreover, the PRF of the GLTD is programmed to match the PRF of the laser designator of the Cobra. Once the GLTD activated the G2 VMIFF device, visibility was reported out to six miles (9.7 km) by the Cobra pilots with estimates from them of visibility in excess of 10 miles (16.1 km). Figure 46 presents images of the G2 VMIFF activated by the GLTD at 300 meters from its position mounted on the top of a building at dusk (left) and during total darkness (right).

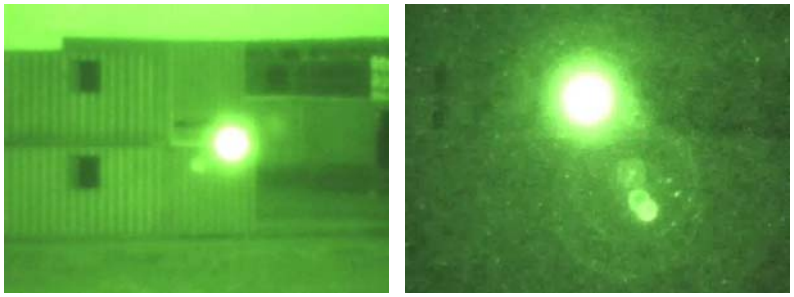

Figure 46. G2 VMIFF Observed at 300 m After Activation by the GLTD at Dusk (left) and During Total Darkness (right).

IV. CONCLUSION AND SUGGESTIONS FOR FURTHER RESEARCH

A. SUMMARY AND CONCLUSION

A practical, operational device has been developed for use by the armed forces to help prevent shooter-on-shooter fratricide in the form of the G3 IIFF patch. Key testing results include:

- Observable at distances in excess of 700 m with image intensifying devices.
- It was discovered that the emitter intensity of both the G2 and G3 patches significantly decreased over a one year period and six month period, respectfully.
- The decrease in emitter intensity is most likely due to a combination of battery drain and moisture in the air affecting the material properties of the P-OLED.
- The patches, when exposed to extreme temperature conditions ranging from -40 ^{0}C to 71 ^{0}C (likely to be encountered in a military operational environment), remained functional and structurally sound.

The VMIFF was designed to prevent low altitude air-to-ground fratricide within a 3 km to 5 km range, corresponding to the range at which a helicopter pilot is able to recognize a target. Key design and testing results include:

- The G1 VMIFF design was scaled to conform to the emission intensity data of the G2 IIFF patch.
- It was discovered that the maximum range of observability of the G1 VMIFF was considerably less than that which was predicted by rudimentary calculations.
- The G2 VMIFF was designed and built by a professional engineer using high power LEDs.
- Remote activation of the G2 VMIFF using a modulated targeting laser was achieved.

- This G2 VMIFF was visible at least out to 6 miles (9.7 km) with estimates of visibility out to 8 miles (12.9 km) as confirmed by the observations of the Cobra pilots from the Yuma, AZ, test.
- An absolute maximum range of observability has yet to be determined for the G2 VMIFF.

Both the IIFF patch and VMIFF are devices designed to mitigate the number fratricide incidents in the complex military machine of today. They are intended to be used as a means of last resort, not as a primary means to replace current target acquisition, identification, and engagement procedures. Ideally, through increased research and testing, these devices will be employed on the battlefield in the near future.

B. SUGGESTIONS FOR FURTHER RESEARCH

As mentioned in Chapter I, most of the emission from the current P-OLED emitter material is in the visible region of the electromagnetic spectrum and is filtered and discarded prior to emission. Research in quantum dot technology will move more of the emission into the near IR, therefore resulting in a brighter patch emission.

Quantum dot (QD) materials are extremely small semiconductor crystals, ranging in size from a few nanometers to a few tens of nanometers, with optical properties that can be tuned, through size modifications, away from their bulk properties to have unique absorption and emission bands [11]. AVI has the ability to incorporate the QD material into thin films, much like the light emitting polymer material (LEP) used in the patches. Using the P-OLED materials combined with QD would permit more of the emission power from the patch to be radiated at IR wavelengths. Therefore, less of the emitted radiation will be discarded and the emission from the patch will be brighter in the near IR per unit of electrical power.

As mentioned above, the purpose of the QD layer down conversion is to shift the emission spectrum of the P-OLED to longer wavelengths in order to allow more of the power from the P-OLED emission to be radiated at near IR

wavelengths. AVI has proposed a method to do this: an extra QD down conversion layer would be added to the existing P-OLED structure. This QD film would be printed or coated onto the flexible P-OLED display comprising the patch (Figure 47).

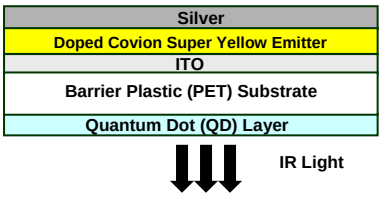

Figure 47. Quantum Dots Down Conversion Process.

The benefits of adding a QD down conversion layer to the existing patch P-OLED structure are numerous. The most obvious benefits are the greatly enhanced visibility and range of the IIFF patches due to a more efficient near IR emitter. Moreover, if the emission were bright enough, the possibility exists for using the P-OLED with QD down conversion for VMIFF displays. The result of this would be light-weight, flexible, and efficient VMIFF displays that draw a relatively small amount of electrical power.

For military application, by tuning the output within the near IR band of frequencies, another version of the IIFF patch could be developed that could be used as a unit specific identifying device for special operations forces conducting covert missions. In such scenarios, each unit member would wear patches that would serve the dual purpose of identifying them as friendly and identifying their unit by a specific sequence of near IR emissions.

THIS PAGE INTENTIONALLY LEFT BLANK

APPENDIX A. MAXIMUM INTENSITY FROM .JPEG IMAGES MATLAB CODE (MAXINTENSITY.M)

```
%MATLAB code to find maximum intensity from monochromator images
Z1=imread('0s_750nmb.JPG')
Z1=double(Z1)
[Y1,X]=max(Z1)
mmx1=max(Y1)
max1=mmx1(:,:,1)
Z2=imread('15s_762nmb.JPG')
Z2=double(Z2)
[Y2,X]=max(Z2)
mmx2=max(Y2)
max2=mmx2(:,:,1)
Z3=imread('30s_774nmb.JPG')
Z3=double(Z3)
[Y3,X]=max(Z3)
mmx3=max(Y3)
max3=mmx3(:,:,1)
Z4=imread('45s_786nmb.JPG')
Z4=double(Z4)
[Y4,X]=max(Z4)
mmx4=max(Y4)
max4=mmx4(:,:,1)
Z5=imread('60s_798nmb.JPG')
Z5=double(Z5)
[Y5,X]=max(Z5)
mmx5=max(Y5)
max5=mmx5(:,:,1)
Z6=imread('75s_810nmb.JPG')
Z6=double(Z6)
[Y6,X]=max(Z6)
mmx6=max(Y6)
max6=mmx6(:,:,1)
Z7=imread('90s_822nmb.JPG')
Z7=double(Z7)
[Y7,X]=max(Z7)
mmx7=max(Y7)
max7=mmx7(:,:,1)
Z8=imread('105s_834nmb.JPG')
Z8=double(Z8)
[Y8,X]=max(Z8)
mmx8=max(Y8)
max8=mmx8(:,:,1)
Z9=imread('120s_846nmb.JPG')
Z9=double(Z9)
[Y9,X]=max(Z9)
mmx9=max(Y9)
max9=mmx9(:,:,1)
Z10=imread('135s_858nmb.JPG')
Z10=double(Z10)
[Y10,X]=max(Z10)
```

```
mmx10=max(Y10)
max10=mmx10(:,:,1)
Z11=imread('150s_870nmb.JPG')
Z11=double(Z11)
[Y11,X]=max(Z11)
mmx11=max(Y11)
max11=mmx11(:,:,1)
Z12=imread('155s_874nmb.JPG')
Z12=double(Z12)
[Y12,X]=max(Z12)
mmx12=max(Y12)
max12=mmx12(:,:,1)
Z13=imread('160s_878nmb.JPG')
Z13=double(Z13)
[Y13,X]=max(Z13)
mmx13=max(Y13)
max13=mmx13(:,:,1)
Z14=imread('165s_882nmb.JPG')
Z14=double(Z14)
[Y14,X]=max(Z14)
mmx14=max(Y14)
max14=mmx14(:,:,1)
Z15=imread('170s_886nmb.JPG')
Z15=double(Z15)
[Y15,X]=max(Z15)
mmx15=max(Y15)
max15=mmx15(:,:,1)
Z16=imread('175s_890nmb.JPG')
Z16=double(Z16)
[Y16,X]=max(Z16)
mmx16=max(Y16)
max16=mmx16(:,:,1)
Z17=imread('180s_894nmb.JPG')
Z17=double(Z17)
[Y17,X]=max(Z17)
mmx17=max(Y17)
max17=mmx17(:,:,1)
Z18=imread('185s_898nmb.JPG')
Z18=double(Z18)
[Y18,X]=max(Z18)
mmx18=max(Y18)
max18=mmx18(:,:,1)
Z19=imread('190s_902nmb.JPG')
Z19=double(Z19)
[Y19,X]=max(Z19)
mmx19=max(Y19)
max19=mmx19(:,:,1)
Z20=imread('195s_906nmb.JPG')
Z20=double(Z20)
[Y20,X]=max(Z20)
mmx20=max(Y20)
max20=mmx20(:,:,1)
Z21=imread('200s_910nmb.JPG')
Z21=double(Z21)
[Y21,X]=max(Z21)
mmx21=max(Y21)
max21=mmx21(:,:,1)
```

```
Z22=imread('205s_914nmb.JPG')
Z22=double(Z22)
[Y22,X]=max(Z22)
mmx22=max(Y22)
max22=mmx22(:,:,1)
Z23=imread('210s_918nmb.JPG')
Z23=double(Z23)
[Y23,X]=max(Z23)
mmx23=max(Y23)
max23=mmx23(:,:,1)
Z24=imread('215s_922nmb.JPG')
Z24=double(Z24)
[Y24,X]=max(Z24)
mmx24=max(Y24)
max24=mmx24(:,:,1)
Z25=imread('220s_926nmb.JPG')
Z25=double(Z25)
[Y25,X]=max(Z25)
mmx25=max(Y25)
max25=mmx25(:,:,1)
Z26=imread('225s_930nmb.JPG')
Z26=double(Z26)
[Y26,X]=max(Z26)
mmx26=max(Y26)
max26=mmx26(:,:,1)
Z27=imread('230s_934nmb.JPG')
Z27=double(Z27)
[Y27,X]=max(Z27)
mmx27=max(Y27)
max27=mmx27(:,:,1)
Z28=imread('235s_938nmb.JPG')
Z28=double(Z28)
[Y28,X]=max(Z28)
mmx28=max(Y28)
max28=mmx28(:,:,1)
Z29=imread('240s_942nmb.JPG')
Z29=double(Z29)
[Y29,X]=max(Z29)
mmx29=max(Y29)
max29=mmx29(:,:,1)
Z30=imread('245s_946nmb.JPG')
Z30=double(Z30)
[Y30,X]=max(Z30)
mmx30=max(Y30)
max30=mmx30(:,:,1)
Z31=imread('250s_950nmb.JPG')
Z31=double(Z31)
[Y31,X]=max(Z31)
mmx31=max(Y31)
max31=mmx31(:,:,1)
Z32=imread('255s_954nmb.JPG')
Z32=double(Z32)
[Y32,X]=max(Z32)
mmx32=max(Y32)
max32=mmx32(:,:,1)
Z33=imread('260s_958nmb.JPG')
Z33=double(Z33)
```

```
[Y33,X]=max(Z33)
mmx33=max(Y33)
max33=mmx33(:,:,1)
Z34=imread('265s_962nmb.JPG')
Z34=double(Z34)
[Y34,X]=max(Z34)
mmx34=max(Y34)
max34=mmx34(:,:,1)
Z35=imread('270s_966nmb.JPG')
Z35=double(Z35)
[Y35,X]=max(Z35)
mmx35=max(Y35)
max35=mmx35(:,:,1)
Z36=imread('275s_970nmb.JPG')
Z36=double(Z36)
[Y36,X]=max(Z36)
mmx36=max(Y36)
max36=mmx36(:,:,1)
Z37=imread('280s_974nmb.JPG')
Z37=double(Z37)
[Y37,X]=max(Z37)
mmx37=max(Y37)
max37=mmx37(:,:,1)
Z38=imread('285s_978nmb.JPG')
Z38=double(Z38)
[Y38,X]=max(Z38)
mmx38=max(Y38)
max38=mmx38(:,:,1)
Z39=imread('290s_982nmb.JPG')
Z39=double(Z39)
[Y39,X]=max(Z39)
mmx39=max(Y39)
max39=mmx39(:,:,1)
Z40=imread('295s_986nmb.JPG')
Z40=double(Z40)
[Y40,X]=max(Z40)
mmx40=max(Y40)
max40=mmx40(:,:,1)
Z41=imread('300s_990nmb.JPG')
Z41=double(Z41)
[Y41,X]=max(Z41)
mmx41=max(Y41)
max41=mmx41(:,:,1)
Z42=imread('305s_994nmb.JPG')
Z42=double(Z42)
[Y42,X]=max(Z42)
mmx42=max(Y42)
max42=mmx42(:,:,1)
Z43=imread('310s_998nmb.JPG')
Z43=double(Z43)
[Y43,X]=max(Z43)
mmx43=max(Y43)
max43=mmx43(:,:,1)
%Matrix for maximum values
X=[max1 max2 max3 max4 max5 max6 max7 max8 max9 max10 max11 max12 max13
max14 max15 max16 max18 max19 max20 max21 max22 max22 max23 max24 max25
```

```
max26 max27 max28 max29 max30 max31 max32 max33 max34 max35 max36 max37
max38 max39 max40 max41]
%Wavelength values for corresponding images
lambda=[750,762,774,786,798,810,822,834,846,858,870,874,878,882,886,890
,894,898,902,906,910,914,918,922,926,930,934,938,942,946,950,954,958,96
2,966,970,974,978,982,986,990]
%Plot creation
plot(lambda,X,'bo')
grid on
xlabel('Wavelength(nm)')
ylabel('Peak Intensity')
title('Intensity vs Wavelength')
```

THIS PAGE INTENTIONALLY LEFT BLANK

APPENDIX B. OPTEK POINT SOURCE INFRARED EMITTING DIODE (TYPE OP265WPS)

Product Bulletin OP265WPS
November 2000

Plastic Point Source Infrared Emitting Diode
Type OP265WPS

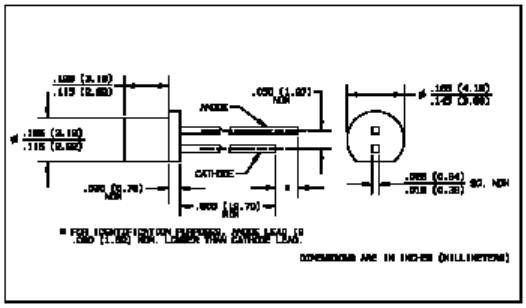

150

Features

- Point source irradiance pattern
- Small package size for space limited applications
- T-1 package style

Description

The OP265WPS is an 850 nm high intensity gallium aluminum arsenide infrared emitting diode molded in an IR transmissive amber-tinted epoxy package. The broad radiation pattern provides relatively even illumination over a large area. The point source GaAlAs IRED emits photons from a 0.004" diameter area centered within the package for precision optical designs. This package is a T-1 style in all respects except for the length of the plastic package.

The stable V_F vs. Temperature characteristic make them ideal for applications where voltage is limited (such as battery operation).

The low t_r/t_f make them ideal for high speed operation.

Absolute Maximum Ratings (T_A = 25° C unless otherwise noted)

Reverse Voltage	2.0 V
Continuous Forward Current	50 mA
Peak Forward Current (2 µs pulse width, 0.1% duty cycle)	1.0 A
Storage and Operating Temperature Range	-40° C to +100° C
Lead Soldering Temperature [1/16 inch (1.6 mm) from case for 5 sec. with soldering iron]	260° C (1)
Power Dissipation	100 mW (2)

NOTES:
(1) RMA flux is recommended. Duration can be extened to 10 seconds maximum when flow soldering. A maximum of 20 grams force may be applied to the leads when soldering.
(2) Derate linearly 1.33 mW/° C above 25° C.
(3) $E_{e(APT)}$ is a measurement of the average apertured radiant incidence upon a sensing area 0.081" (2.06 mm) in diameter, perpendicular to and centered on the mechanical axis of the lens, and 0.590" (14.99 mm) from the measurement surface. $E_{e(APT)}$ is not necessarily uniform within the measured area.

Optek Technology, Inc. 1215 W. Crosby Road Carrollton, Texas 75006 (972) 323-2200 Fax (972) 323-2396

THIS PAGE INTENTIONALLY LEFT BLANK

APPENDIX C. MARUBENI L850F-06-55 INFRARED LED LAMP FOR HIGH CURRENT DRIVE

Marubeni

L850F-06-55 Infrared LED Lamp for High Current Drive

L850F-06-55 is an AlGaAs LED mounted on a lead frame with a clear epoxy lens.
On forward bias, it emits a spectral band of radiation which peaks at 850nm. These devices are intended to be operated at pulsed current of 2A under maximum 4.3V for stable long life.

♦Specifications

1)Product Name	Infrared LED Lamp
2)Type No.	L850F-06-55
3)Chip	
(1)Chip Material	AlGaAs
(2)Chip Dimension	550umx550um
(3)Peak Wavelength	850nm typ.
4)Package	
(1)Type	Φ5mm clear molding
(2)Resin Material	Epoxy Resin
(3)Lead Frame	Soldered

♦Outer dimension(Unit: mm)

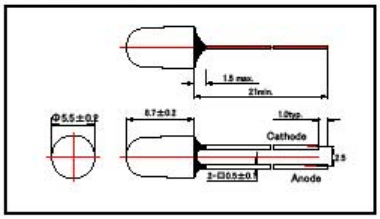

♦Absolute Maximum Ratings

Item	Symbol	Maximum Rated Value	Unit	Ambient Temperature
Power Dissipation	PD	150	mW	Ta=25°C
Forward Current	IF	100	mA	Ta=25°C
Pulse Forward Current	IFP	2000	mA	Ta=25°C
Reverse Voltage	VR	5	V	Ta=25°C
Operating Temperature	TOPR	-30 ~ +85	°C	
Storage Temperature	TSTG	-30 ~ +100	°C	
Soldering Temperature	TSOL	260	°C	

‡Pulse Forward Current condition: Duty=1% and Pulse Width=10us.
‡Soldering condition: Soldering condition must be completed within 3 seconds at 260°C

♦Electro-Optical Characteristics [Ta=25°C]

Item	Symbol	Condition	Minimum	Typical	Maximum	Unit
Forward Voltage	VF/VFP	IF=50mA DC		1.42	1.50	V
		IFP=1A		3.2	3.5	
		IFP=2A		3.6	4.3	
Reverse Current	IR	VR=5V			10	uA
Total Radiated Power	PO	IF=50mA DC	18.0	20.0		mW
		IF=100mA, tp=20ms		40.0		
Radiant Intensity	IE	IF=50mA DC	90	120		mW/sr
		IF=100mA, tp=20ms		240		
Peak Wavelength	λP	IF=50mA DC	840	850	860	nm
Half Width	Δλ	IF=50mA DC		40		nm
Viewing Half Angle	θ 1/2	IF=50mA DC		±8		
Rise Time	tr	IF=50mA DC		15		ns
Fall Time	tf	IF=50mA DC		10		ns

‡Total Radiated Power is measured by Photodyne #500
‡Radiant Intensity is measured by Tektronix J-6512.

Marubeni America Corporation
3945 Freedom Circle, Suite 1000, Santa Clara, CA 95054
408-330-0650 (Ext. 323), 408-330-0655 (Fax), sales@tech-led.com

THIS PAGE INTENTIONALLY LEFT BLANK

APPENDIX D. COMPLETE CIRCUIT SCHEMATIC OF G2 VMIFF

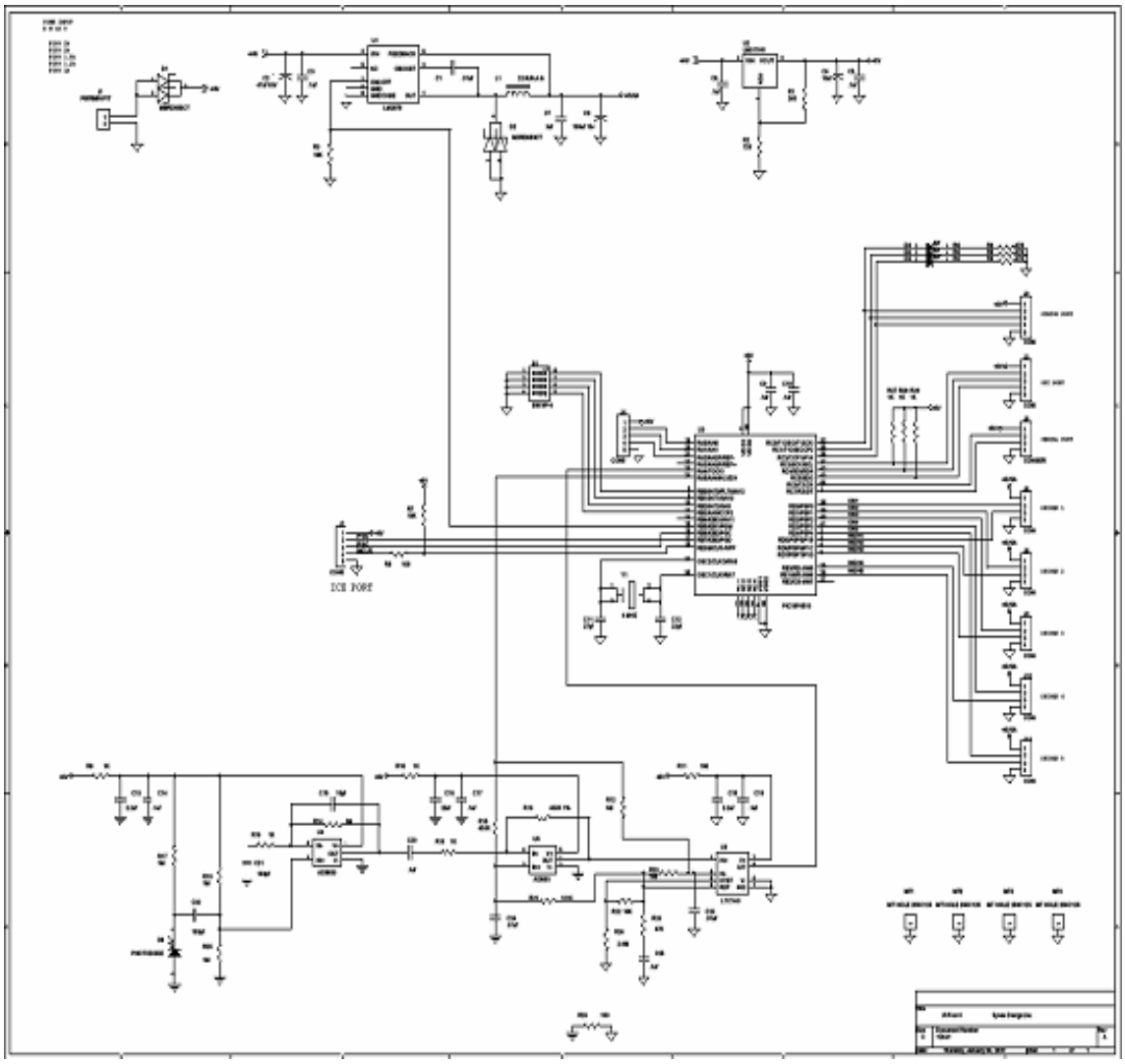

THIS PAGE INTENTIONALLY LEFT BLANK

LIST OF REFERENCES

[1] E. Downing, (2007, January 23). *Friendly fire*. Retrieved January 30, 2007, from http://www.answers.com/topic/friendly-fire

[2] M.E. Mullen, (1996, November 11). *The American Friendly-Fire Notebook.* Retrieved January 23, 2007 from http://members.aol.com/amerwar/ff/ff.htm

[3] David H. Hackworth, (1991, November 18). Killed by Their Comrades. *Newsweek*, 45.

[4] Amanda Bower, (2003, April 7). Misfiring in the Fog. *Time*, 161, 39.

[5] Dale Eisman, (2004, May 1). U.S. Forces Still Struggle to Tell Friend from Foe. *The Virginian-Pilot*, p. A1.

[6] Marine Corps Base, Camp Lejeune, N.C. (2006, May 1). *Optics Systems.* Retrieved 31 January 2007 from http://www.lejeune.usmc.mil/lmt/downloads/Target%20Acquisition%20Systems%20Devices%20_May%202006_.pdf

[7] Add-Vision, Inc. (2007). *Add-Vision's Display Technology.* Retrieved 6 March 2007 from http://www.add-vision.com/display_technology.php

[8] IFF Technology Investigation Defense Acquisition Challenge (DAC) Final Report, (2007, February 1). *LVC Corporation*. Natick, MA: U.S. Special Operations Command PM, SOF Survival Systems.

[9] Headquarters, United States Marine Corps, (1995, December 5). *AH-1W Super Cobra Helicopter.* Retrieved 14 February 2007 from http://www.hqmc.usmc.mil/factfile.nsf

[10] Air Naval Tactics, Techniques, and Procedures, (2005). *Combat Aircraft Fundamentals: AH-1(U) (Navy Warfare Development Command Publication Air NTTP 3-22.3-AH1W)*. Yuma, AZ: Marine Aviation Weapons and Tactics Squadron One.

[11] FYO7 Partnership Proposal for MASINT Consortium, (2006). *Development of Remotely Interrogated IR Polymer Emitters for IIFF (Individual Identify Friend or Foe) and Associated Covert Applications*. NMCR Tracking # 10P07AVI_NPSMack**.** Monterey, CA: Naval Postgraduate School.

[12] M. Bayindir, & F. Sorin & A.F. Abouraddy, & J. Viens, & S.D. Hart, & J.D., Joannopoulos, et al., (2004, October 14). Metal-insulator-semiconductor optoelectronic fibres. *Nature*, 431, 826-829.

[13] F.L. Pedrotti, & L.S. Pedrotti, & L.M. Pedrotti, (2007). *Introduction to Optics.* Upper Saddle River, NJ: Pearson Prentice Hall.

[14] S.O. Kasap, (2001). *Optoelectronics and Photonics, Principles and Practices.* Upper Saddle River, NJ: Pearson Prentice Hall.

[15] S.O. Kasap, (2002). Pr*inciples of Electronic Materials and Devices.* New York: McGraw-Hill.

[16] P. Horowitz, & W. Hill, (1988). *The Art of Electronics.* New York: Cambridge University Press.

[17] D. Hansdlman, & B. Littlefield, (2005). *Mastering MATLAB.* Upper Saddle River, NJ: Pearson Prentice Hall.

INITIAL DISTRIBUTION LIST

1. Defense Technical Information Center
   Ft. Belvoir, Virginia

2. Dudley Knox Library
   Naval Postgraduate School
   Monterey, California

3. Professor James H. Luscombe
   Naval Postgraduate School
   Monterey, California

4. Professor Nancy M. Haegel
   Naval Postgraduate School
   Monterey, California

5. Professor Richard M. Harkins
   Naval Postgraduate School
   Monterey, California

6. Captain Patrick S. Williams, USMC
   Naval Postgraduate School
   Monterey, California

7. CDR F. Mitchell Bradley, USN
   JSOC
   Fort Bragg, North Carolina

8. Major Jeffrey Dunn, USMC
   Marine Corps Warfighting Laboratory
   Quantico, Virginia

9. Lucius “Gus” Taylor IV
   Program Manager USSOCOM SOPMOD
   NSWC Crane
   Crane, Indiana